MAKERERE UNIVERSITY

COLLEGE OF AGRICULTURAL AND ENVIRONMENTAL SCIENCES

SCHOOL OF FOOD TECHNOLOGY, NUTRITION AND BIOENGINEERING

DEPARTMENT OF AGRICULTURAL AND BIO-SYSTEMS ENGINEERING

DEVELOPMENT AND PERFORMANCE ASSESSMENT OF A SOLAR-POWERED VACCINE REFRIGERATION SYSTEM FOR OFF-GRID RURAL HEALTH FACILITIES

Presented by:

LOKONG PETER

REGISTRATION NUMBER:

22/U/6229

STUDENT NUMBER:

2200706229

SUPERVISORS:

PROF. NICHOLAS KIGGUNDU

DR. NAKAWUKA PROSSIE

A THESIS SUBMITTED TO THE DEPARTMENT OF AGRICULTURAL AND BIOSYSTEMS ENGINEERING IN PARTIAL FULFILLMENT OF THE REQUIREMENTS FOR THE AWARD OF BACHELOR OF SCIENCE IN AGRICULTURAL ENGINEERING

JUNE 2026

DECLARATION

DECLARATION

I, LOKONG PETER, state that this project report, titled "Development and Performance Assessment of a Solar-Powered Vaccine Refrigeration System for Off-Grid Rural Health Facilities," is my own original work. I have not submitted it to any higher education institution for any academic degree. All sources used in this report have been properly acknowledged.

STUDENT'S NAME: LOKONG PETER

REGISTRATION NUMBER: 22/U/6229

Signature: [illegible]

Date: 31/07/2026

ii

APPROVAL

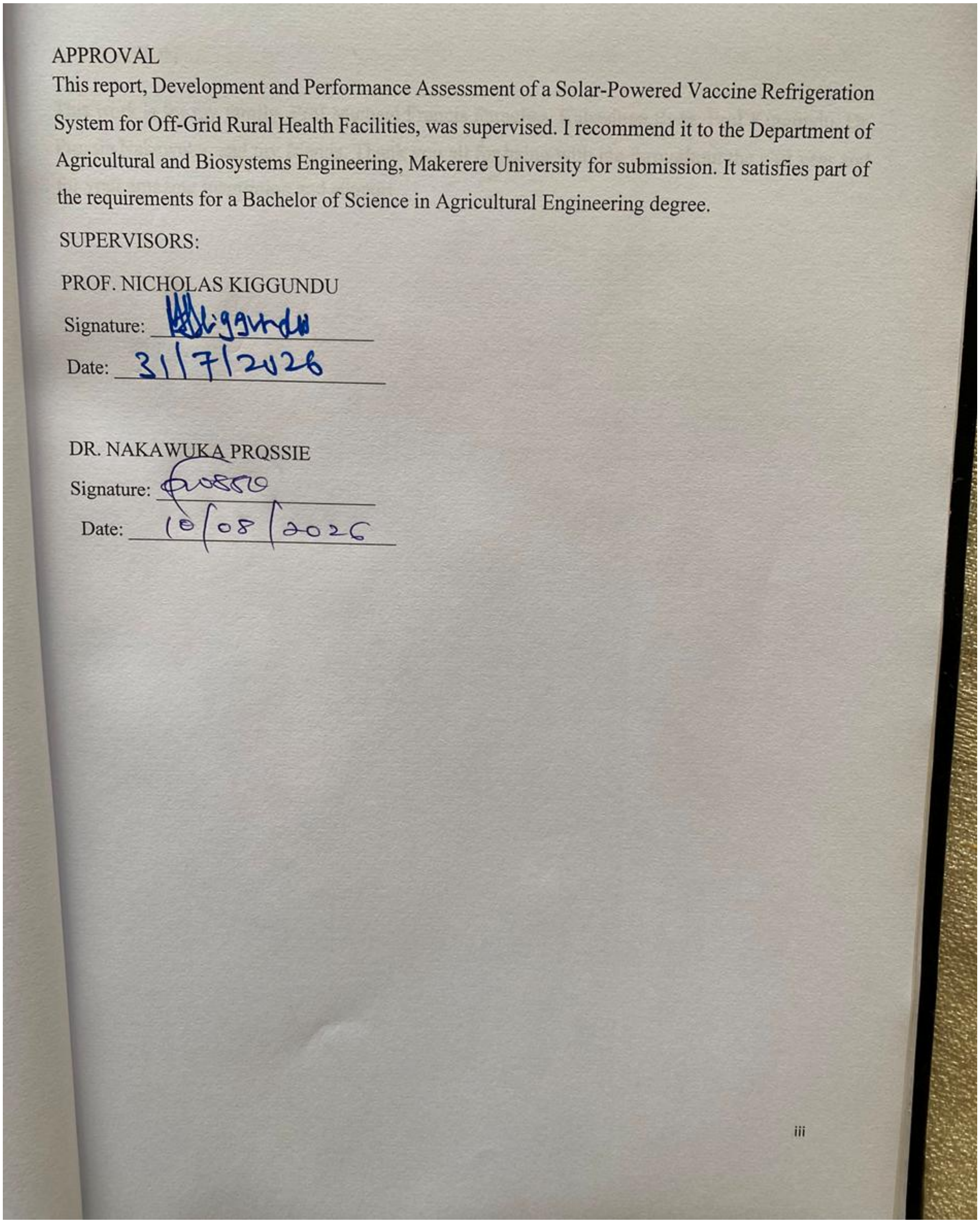

APPROVAL

This report, Development and Performance Assessment of a Solar-Powered Vaccine Refrigeration System for Off-Grid Rural Health Facilities, was supervised. I recommend it to the Department of Agricultural and Biosystems Engineering, Makerere University for submission. It satisfies part of the requirements for a Bachelor of Science in Agricultural Engineering degree.

SUPERVISORS:

PROF. NICHOLAS KIGGUNDU

Signature: ____________

Date: 31/7/2026

DR. NAKAWUKA PROSSIE

Signature: ____________

Date: 10/08/2026

iii

DEDICATION

This work is for my family, Prof Michael Francis Faragher, Kabasinga Rose, Prof Kiggundu, Dr. Prossie Nakawuka, and my friends. Thank you all for being with me throughout the past year and for your amazing inspiration and support.

ACKNOWLEDGEMENT

Finally, I must thank God for His giving of the wisdom, health, and strength for my being able to finalize and accomplish this. Finally, my sincere thanks go to my supervisors. Prof. Nicholas Kiggundu and Dr. Nakawuka Prossie.

They provided important guidance, mentorship, and helpful feedback as we designed and developed this solar-powered vaccine refrigerator.

I also extend my gratitude to the staff and colleagues of the Department of Agricultural and Biosystems Engineering, as well as to my family, for their moral and financial support throughout this research journey, and most especially Prof. Michael Francis Faragher from Liverpool John Moores University for his continuous support towards accomplishing my project.

Contents

List of Tables

List of figures

LIST OF ABBREVIATIONS

Abbreviation	Full Meaning
AC	Alternating Current
ANOVA	Analysis of Variance
ASHRAE	American Society of Heating, Refrigerating and Air-Conditioning Engineers
COP	Coefficient of Performance
CO_2	Carbon Dioxide
DC	Direct Current
DHT22	Digital Temperature/Humidity Sensor
EER	Energy Efficiency Ratio
EL	Electrical Load
ARDUINO UNO	ATmega328P-based microcontroller board.
GHG	Greenhouse Gas
GWP	Global Warming Potential
HC	Hydrocarbon
HCFC	Hydrochlorofluorocarbon
HFC	Hydrofluorocarbon
HOMER	Hybrid Optimization Model for Electric Renewables
HT	Average Daily Solar Insolation
IEC	International Electrotechnical Commission
ISO	International Organization for Standardization
kWh	Kilowatt-hour
LCC	Life-Cycle Cost
LCOE	Levelized Cost of Energy
$LiFePO_4$	Lithium Iron Phosphate Battery
MPPT	Maximum Power Point Tracking
NASA	National Aeronautics and Space Administration
NH_3	Ammonia
ODP	Ozone Depletion Potential
PCM	Phase Change Material
PQS	Performance, Quality and Safety (WHO standard)
PV	Photovoltaic
QL	Cooling Load
Qevap	Heat Absorbed in the Evaporator
R134a	Tetrafluoroethene (Synthetic Refrigerant)
R290	Propane (Natural Refrigerant)
R600a	Isobutane (Natural Refrigerant)
R717	Ammonia Refrigerant

Abbreviation	Full Meaning
R744	Carbon Dioxide Refrigerant
SDD	Solar Direct Drive
SOC	State of Charge
SRI	System Reliability Index
TDI	Temperature Deviation Index
TEWI	Total Equivalent Warming Impact
UNMA	Uganda National Meteorological Authority
UNICEF	United Nations Children's Fund
WHO	World Health Organization
Wcomp	Compressor Work

ABSTRACT

Safe vaccine storage – vaccine efficacy depends on a safe cold chain. However, many rural and off-grid healthcare centres in Uganda suffer from frequent power crises, high cost of energy, as well as lack of proper cold chain equipment and infrastructure. Consequently, in order to keep safe storage conditions (between 2 and 8 °C) and to lessen dependence on electricity and the cost of cooling with low environmental impact, we developed a 50-litre solar refrigerator. This concept integrates 50 W of solar PV, a 100 Ah battery, grid back-up and a 50 W vapor compressor using R290 (propane). The use of R290 was chosen as part of the move to refrigerants which do not negatively impact climate change. R290 has a Global Warming Potential (GWP) of roughly 3 as opposed to1,430 for R134a. The system was tested in Busamuzi Health Centre II, Buvuma District. We recorded temperatures with an Arduino every 15 minutes. I also employed thermodynamic simulation, statistical analysis, and a Total Equivalent Warming Impact assessment. This device kept the internal temperature stable at an average 4.1C. The average value fluctuated between 3.8 and 4.4C most of the time. The Stability Reliability Index value is 96.8%, as, after achieving the target temperature, the value never fell outside 2- 8 °C. The steady-state COP was 5.80, much better than the target of 3.0 of the study. It used around 468 watt-hours per day. The statistics showed that the real performance was significantly different from the performance of our simulation ($p < 0.05$). Simulations also showed that refrigerants behave very differently. The system took 165 minutes to reach the desired storage temperature, which was above the target of 120 minutes. The results overall indicate that the combination of solar power, a 100 Ah battery, a grid power option, and R290 refrigeration is a good way to improve vaccine cold storage in rural areas, especially given the low environmental impact of the system. Recommend adjustingcompressors sizeand Insulation with some more test cases of hot conditions, safety, and certification for mass production.

Keywords: Solar-powered refrigeration; Vaccine cold chain; R290 propane; Natural refrigerants; COP; Solar PV; Battery storage; TEWI; Rural healthcare; Uganda.

CHAPTER ONE: INTRODUCTION

1.1. BACKGROUND

A major problem that we face in much of the developing world, particularly in isolated rural areas, is a lack of access to suitable refrigeration where power systems can be unreliable or non-existent. This is most critical in the healthcare sector where refrigeration must be consistent for the storing of vaccines, drugs, and many other medical supplies. (WHO, 2020). Every year, at least a quarter of the world's vaccines end up getting wasted due to poor cold-chain facilities (WHO and UNICEF, 2014). Africa, particularly in areas in Sub-Saharan Africa where power access and reliable equipment still lag behind (Lahnaoui et al., 2024).

Vaccines: biological products that need to be kept cold. Biological products that are highly sensitive to both heat and cold, like vaccines, require strict adherence to storage and handling of their narrow target storage temperature of 2–8 C to protect them and maximize their efficacy (WHO, 2024). The cold chain is a critical link that is fragile. When vaccines travel through vast rural and isolated communities where regular grid electricity is elusive, keeping them cold can be daunting. Interruptions in electricity supply, soaring costs of power, and reliance on fuel-dependent devices have meant lost stock, lapsed inoculations, and major obstacles to health and immunization programs (Izuka et al., 2023).

The majority of refrigeration systems are based on Grid electricity with high GWP HFCs as working refrigerants. Facing the challenge from human-made emissions the system there has been much work done in developing Alternative Refrigeration in the field of natural refrigerants such as NH3, Propane, CO2, and HCs, which have zero ODP and low GWP.(Arabi et al., 2024).

Solar Refrigeration: a sustainable approach. Solar-powered refrigeration provides a sustainable and efficient solution that can also be a sustainable alternative by leveraging the massive sunshine available (approx 5-6 kWh per m^2 per day), especially in solar-rich environments, as is the case in Uganda, where renewable energy generation. Health facilities could then easily implement and ensure access to safe cold vaccines and medications without being subject to unreliable grid (McCarney et al., 2013; Zhao et al., 2023). Recent studies and pilot projects in Africa and Asia demonstrate that solar-powered refrigerators using natural refrigerants are not only technically feasible but also economically viable in the long run, given reductions in operational costs and alignment with global climate goals (Garcia et al., 2025).

The project will propose to design and construct a solar-powered refrigerator for use at the Health facility by incorporating the use of natural refrigerants thus enhancing sustainability and health safety associated with the use of a refrigerator. The project will address the issues of energy access and climate change in two ways in order to ensure quality healthcare while also ensuring that green energy is utilized efficiently.

1.2. PROBLEM STATEMENT

However, the Ugandan villages still have a significant deficit in the level of electrical energy, causing the clinics to experience difficulties in coping with the power failures that occur occasionally and threaten to damage the stock of various vaccines. Solar energy can be considered as a viable solution in this case, but the existing solar powered refrigerators are expensive, underpowered, and utilize synthetic refrigerants. Solar powered refrigerators that use natural refrigerants can offer an affordable, reliable, and eco-friendly solution to the problem, but they have not been implemented yet. Since health facilities are the pillars of primary healthcare, the negligence of their needs leads to the deterioration of a wide range of services, such as vaccination, medication storage, and others, putting the population at risk. As a result, the researchers proposed to develop a solar-powered vaccine refrigerator. It would use natural refrigerants, including propane, carbon dioxide, water, and utilize a battery (lead-acid or lithium-ion), ensuring the uninterrupted flow of electricity. Furthermore, the device would be constructed in such a way that it could operate in an area without access to the main electricity supply and would be easy to maintain and equipped with temperature control, thus being able to meet the needs of the population and help ensure the proper organization of a vaccination campaign, as well as the general improvement of the healthcare service, for Health Centre II communities.

1.3. RESEARCH OBJECTIVE

Growing demand for reliable cold storage in rural health centres, which have been constrained by unreliable grid electricity supply, high capital costs of conventional cold chain equipment, and the unfriendly environmental impact of synthetic refrigerants, has prompted the need to develop more efficient, affordable, and environmentally safe solar cold chain systems.

Although solar-powered refrigeration systems are a viable alternative, the technology has faced challenges in terms of performance, cost, and versatility in diverse applications. This study therefore sought to develop and evaluate an affordable, energy-efficient, and reliable solar power refrigerator for vaccine storage in rural health facilities

MAIN OBJECTIVE

To Design, construct, and evaluate a sustainable, affordable, eco-friendly solar-powered vaccine refrigeration system using R290 natural refrigerant, targeting full compliance with the WHO PQS E003 Performance Standards

SPECIFIC OBJECTIVES

I. To design a 50-litre vaccine refrigeration system, which will utilize R290 as a natural refrigerant with thermal performance passing the World Health Organization Performance Qualification standard for Vaccine Storage (WHO-PQS-E003) applicable for off-grid vaccine storage in Rural Health Facilities.

II. To construct and assemble the designed vaccine refrigeration systems by sourcing all components locally from Uganda. Using appropriate components such as photovoltaic panels, Battery Storage, etc., in sizes corresponding to the design load.

III. To evaluate technical parameters (Temperature stability 2-8°C, SRI≥95%, TDI<1.5°C, Pull Down Time <120 min, Coefficient of Performance COP> 3.0), Economic Evaluation (Lifecycle Cost Compared to Diesel Baseline), and Environmental Impact.

1.4. RESEARCH HYPOTHESIS

The following hypothesis guides this study:

H_1 (Alternative Hypothesis):

Solar-powered R290 refrigeration significantly improves vaccine storage reliability (WHO temperature stability, pull-down time, COP), economic viability (lower lifecycle cost), and environmental impact (lower TEWI) compared to conventional systems.

H_0 (Null Hypothesis):

Solar-powered R290 refrigeration does not significantly improve reliability, economic viability, or environmental impact compared to conventional systems.

1.5. CONCEPTUAL FRAMEWORK

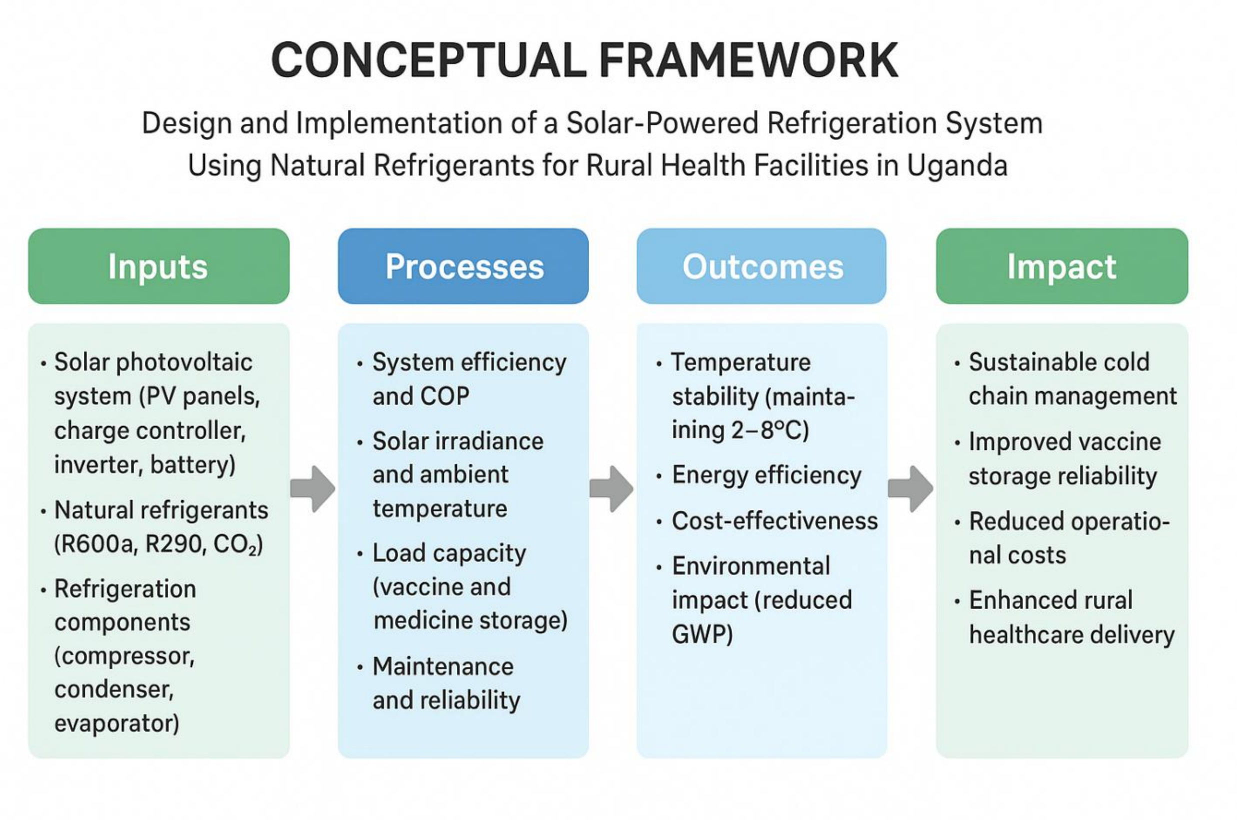

Figure 1. Conceptual framework

1.6. Justification

Reliable refrigeration is a cornerstone in healthcare delivery, particularly for vaccines, medicines, and other temperature-sensitive health products. In Uganda, many rural health facilities are off-grid or suffer frequent power interruptions, impairing proper cold storage and undermining vaccine potency and health outcomes. According to a root-cause analysis of failed cold chain equipment in Uganda, refrigerant leaks, power failures, and maintenance issues are significant contributors to system breakdowns.(Path, 2016).

Solar energy offers a viable solution in such contexts. Projects by UNICEF and Uganda's Ministry of Health are adopting solar refrigerators to strengthen the cold chain: as of late 2024, Uganda had procured over 550 solar refrigerators to extend cold chain capacity in remote areas (Ministry of Health, 2025; UNICEF, 2024). Moreover, studies have shown that solar PV systems can reliably power vaccine refrigeration in remote health facilities, though battery life and system design remain key challenges. However, most existing systems continue to use synthetic refrigerants (HFCs/HCFCs), which contribute significantly to global warming. The transition to natural refrigerants such as hydrocarbons and CO2 is both an environmentally responsible move and increasingly feasible due to case studies/reviews showing it is technically and financially viable for use in solar refrigeration if accompanied by appropriate design of the systems10-15. This research therefore seeks to contribute towards filling a critical void by developing a small scale, solar powered refrigeration system employing natural refrigerants which will deliver a sustainable, low carbon, reliable cold storage solution accessible to rural health facilities while offering additional environmental and economic benefits including cost savings on operational expenses, enhanced energy independence, lower emission outputs and provision of a replicable technology platform scalable from household applications through to agri-cold chain solutions for other underserved populations.

1.7. Scope of the Study

A detailed description of the objective and scope of the research study:

Objective: Design, implement, and evaluate a solar-powered refrigeration system that uses natural refrigerants to meet the cooling requirements of rural health facilities in Uganda.

Scope:

- Technical design of the solar refrigeration system, Load estimation based on usage patterns, Component sizing (e.g., size and number of solar panels, battery capacity, compressor type and size, and refrigerant cycle), Material selection appropriate for tropical climates
- Development and testing of prototypes under controlled conditions, Temperature control within a specified range (2-8°C), Energy consumption during operation, System reliability for vaccine and medicine storage
- Evaluation of the system's technical, economic, and environmental performance compared to existing electric refrigeration systems, financial analysis of costs involved, Environmental impact assessment through reduced greenhouse gas emissions due to the utilization of natural refrigerants

This work has been restricted to studying refrigeration units of small and medium capacities (50 – 150 liters), which are normally utilized in rural health centres. Additionally, there was no need to consider utilizing large-scale cold storage facilities nor full-blown commercial production.

The realization of this project has been carried out at the prototype stage, using simulation tools like Coolselector2, PVSYST, and MATLAB, among others. For instance, we did field testing in the simulator setup in order to determine its performance when actually applied in the field. In addition, some performance tests were done using the code written in VS Code by doing python debugging. We therefore feel confident that our research provides a good model that could easily be replicated within Uganda’s rural areas or anywhere else alike.

CHAPTER 2: LITERATURE REVIEW

2.1 Introduction

In this chapter, an overview of the existing body of knowledge relating to the use of solar-powered refrigeration systems is provided. A special focus is given to vaccine cold chain applications under the conditions typical of those found in off-grid rural healthcare settings. The variety of solar refrigeration technology options is outlined along with details regarding the operation of each, together with associated performance and influencing factors affecting efficiency. Quality parameters set out by the World Health Organisation (WHO) for vaccine storage equipment are described alongside comparative assessments of both natural and synthetic refrigerants. Finally, design protocols have been identified which are established as being currently acceptable practice.

2.2 The Global Challenge of Vaccine Cold Chains

Solar-powered vaccine refrigerators using natural refrigerants represent a critical advancement for rural health facilities, particularly in regions like Uganda, where access to a reliable electricity grid is limited (E. de S. Garcia et al., 2024a; Miyingo et al., 2025; Opoku et al., 2020a) . Approximately 760 million people worldwide lack access, with a significant portion residing in developing countries, facing challenges in storing medicines and vaccines (E. de S. Garcia et al., 2024a). In Uganda, over 80% of rural inhabitants do not have access to electricity (Miyingo et al., 2025). Large-scale immunisation can prevent between 4 and 5 million deaths annually, most related to children up to 5 years old. Most temperature-sensitive vaccines require a controlled temperature between 2.0 °C and 8.0 °C (WHO, 2024). These constraints present a worldwide challenge for cold chain stakeholders, mainly in developing countries where the lack of cooling infrastructure and electricity access can endanger vaccine conservation and distribution (Nadimuthu & Victor, 2021). Only about 34% of hospitals in sub-Saharan Africa currently have reliable electricity access (Sinnei et al., 2023). In Uganda, an unpredictable and unreliable mixed push-pull delivery system often leads to poor vaccine management, stock-outs, and missed vaccination opportunities (Bakkabulindi et al., 2024). Studies in rural Ugandan districts such as Mukono and Kalungu have estimated vaccine wastage rates and assessed contributing factors, emphasizing the need for improved cold chain management (Ninsiima et al., 2025). For example, vaccine hesitancy among both health workers and communities, often informed by concerns around vaccine safety, inaccessibility, and mistrust of authorities, is another concern that could be mitigated by ensuring reliable vaccine delivery systems (Kiptoo et al., 2024; Ouni et al., 2023; Rujumba et al., 2021). Among these categories, “Vaccine safety” emerged as the most important one that accounted for 160 cases, then came “Inaccessibility of Vaccines” with 42, and finally, “Mistrust of gov’t & health authorities” accounting for 33 (Kiptoo et al., 2024).

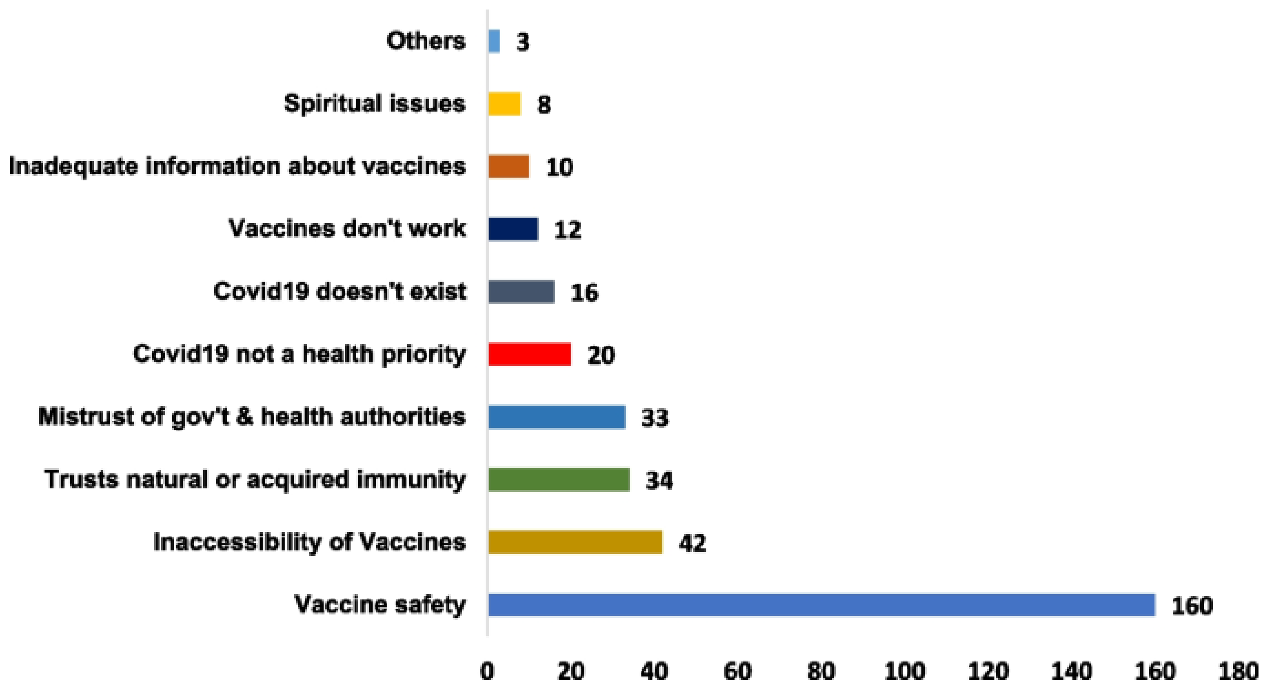

Figure 2. Reasons for Vaccine

Source: (Kiptoo et al., 2024)

Reliability of vaccine cold chain is pivotal to ensuring vaccine potency/efficacy. Any malfunction could spell out massive vaccine wastage with resultant adverse impact on immunisation programme. (Ninsiima et al., 2025; Pambudi et al., 2022; Sinnei et al., 2023). Most traditional refrigeration systems rely on grid supply of electricity and use synthetic refrigerant having high global warming potential. (Sulaiman et al., 2023). There is an ever-increasing concern over climate change and environmental sustainability, which has spurred research activity towards finding alternate refrigeration solutions (Arabi et al., 2024). Amongst others, solar photovoltaic (PV) systems provide a viable and environmentally-friendly solution to many of today’s problems related to refrigeration technologies (E. de S. Garcia et al., 2024b; Raihan Uddin et al., 2021a).

2.3 Types of Solar-Powered Refrigeration Systems

A variety of solar technologies exist with differing advantages and limitations all aimed at converting solar energy to achieve a cooling effect through various unique thermodynamic processes (Chavda et al., 2024)

2.3.1 Vapour Compression Refrigeration (VCR) Systems

Vapour compression systems are the most widely used refrigeration technology for vaccine storage (McCarney et al., 2013). They operate on a mechanical compression cycle using a compressor to circulate refrigerant through a closed loop consisting of four stages: compression, condensation, expansion, and evaporation (ASHRAE, 2021). The compressor raises the pressure and temperature of the refrigerant vapour, which then releases heat in the condenser, expands through an expansion device, and absorbs heat in the evaporator to produce the cooling effect (Raihan Uddin et al., 2021b)

Solar VCR systems can be powered directly by PV panels through a battery system or, in the case of Solar Direct Drive (SDD) systems, without a battery (Maiorino et al., 2025a). An innovative prototype described by (Maiorino et al., 2025a) Used a 160 W solar panel with Maximum Power Point Tracking (MPPT) technology, a lead-acid battery, and a refrigerator using R290 natural refrigerant. The key innovation lay in the use of phase change materials (PCMs), specifically water, to maintain stable temperatures and extend the system's autonomy without external power.

2.3.2 Solar Direct Drive (SDD) Refrigerators

Solar Direct Drive refrigerators are VCR systems designed to run directly from solar PV panels without a battery or inverter (Kapuria et al., 2024a). They use a variable-speed DC compressor that adjusts its speed according to available solar power. SDD systems are becoming popular for vaccine storage because they are robust and reduce battery costs (Kapuria et al., 2024a).

UNICEF procures solar direct-drive refrigeration equipment primarily for the storage of vaccines used in areas without electricity (UNICEF, 2024). The WHO-PQS prequalified SDD systems meet performance requirements with a solar radiation reference period of 3.5 kWh/m²/day and hot zone test temperatures of +43 °C (WHO, 2023).

Field evidence from Kenya demonstrates the transformative impact of SDD refrigerators. At Yapha Dispensary in Kwale County, a solar direct-drive refrigerator was installed in a health centre with no grid electricity. Within one month of delivery, child immunisation rates doubled and continued to rise (Opoku et al., 2020b). The economic prosperity and technological growth of a country are heavily dependent on energy security, and solar energy provides a viable alternative where power is costly, unreliable, or unsustainable (Kaira et al., 2022). The transition to solar direct-drive (SDD) refrigerators is seen as an effort to move towards clean and green energy-driven primary healthcare, addressing both energy and environmental crises (Kapuria et al., 2024b).

2.3.3 Thermoelectric Refrigeration (Peltier Effect)

Thermoelectric refrigerators are based on the Peltier effect, where an electric current passing through a junction of two dissimilar conductors creates a temperature (khan et al., 2023). These systems have no moving parts, are silent, and highly reliable, but their cooling efficiency is low, typically with a COP of 0.5–1.5 (A. A. Khan et al., 2022;Choudhary & Mahto, 2021a)

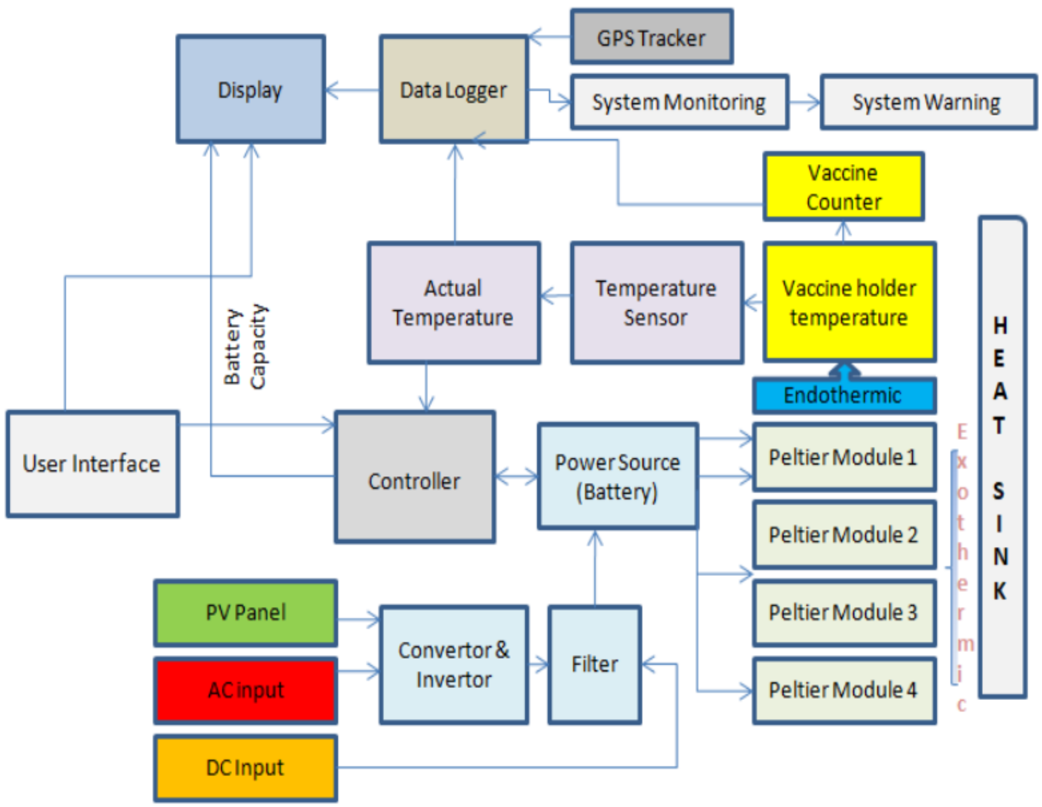

(Source: N. R. Khan et al., 2023)

Thermoelectric systems are being considered for portable medical coolers in remote, off-grid areas (Mehenge et al., 2023a). However, their performance is more affected by ambient temperature than vapour compression systems (Taywade & Wadaskar, 2022).

2.3.4 Absorption Refrigeration Systems

Absorption refrigeration systems use heat (from solar thermal collectors, biomass, or waste heat) to drive the refrigeration cycle, typically employing a water-ammonia or lithium-bromide solution (Mezher et al., 2023). They can operate without electricity but require high-temperature heat input (Mezher et al., 2023). Absorption, compression and thermoelectric types have been compared for vaccine storage applications; a 40 L refrigerator typically requires approximately 1.3 m^2 of photocells for absorption or compression types (Chavda et al., 2024)

2.4 Natural Refrigerants and Environmental Impact

2.4.1 The Problem with Synthetic Refrigerants

Conventional refrigerants such as R134a (tetrafluoroethene) have high Global Warming Potential (GWP) (de Paula et al., 2020) R134a has a GWP of 1,430, meaning that one kilogram of R134a released into the atmosphere has the same warming effect as 1,430 kilograms of carbon dioxide over 100 years (de Paula et al., 2020). Furthermore, the Kigali Amendment to the Montreal Protocol requires the progressive reduction of HFC imports starting in 2024, making R134a-based systems a regulatory liability for long-term investments (NEMA, 2022).

2.4.2 Natural Refrigerants

Natural refrigerants such as propane (R290), isobutane (R600a), ammonia (R717), and carbon dioxide (R744) are increasingly promoted as eco-friendly substitutes due to their negligible ozone depletion potential (ODP) and low GWP (Arabi et al., 2024). R290 has a GWP of 3, an ODP of 0, excellent thermodynamic properties, a low boiling point of −42.1 °C, and an A3 flammability class requiring safety measures (de Paula et al., 2020; Naskar & Mandal, 2024). The R600a has a GWP value of 4 with a slight edge over the R290 in terms of COP for some operating conditions as well. But, on the contrary, this refrigerant possesses a boiling point of -11.7 °C which is comparatively higher than R290 (Raihan Uddin et al., 2021c).

2.4.3 Performance Comparison of Refrigerants

Studies comparing R134a, R32, and R290 refrigerants working in a vapour compression system proved superior thermodynamic and exergy efficiency for the R290 refrigerant covering a wide range of evaporator temperatures (de Paula et al., 2020).

R600a yields the highest COP among hydrocarbons in many conditions due to its lower compression ratio (Raihan Uddin et al., 2021c). However, R290 was selected for many prototypes because of its lower refrigerant charge mass requirement (~60 g vs ~55 g comparable), wider compressor compatibility, greater market penetration in refrigeration service networks, and more stable performance at low evaporating temperatures in hot ambient conditions (J. Garcia et al., 2025; Naskar & Mandal, 2024).

2.5 Factors Affecting the Efficiency of Solar Vaccine Refrigerators

The performance of a solar vaccine refrigerator can be affected by various related factors that need to be accounted for during its design and operation. (McCarney et al., 2013; Raihan Uddin et al., 2021c)

2.5.1 Ambient Temperature

For example, higher ambient temperature will increase the condensing pressure as well as the compressor's work while decreasing COP (Raihan Uddin et al., 2021). The design must be based on the highest expected ambient temperature to allow adequate cooling under worst-case scenarios. WHO PQS E003 states that this test should be carried out at a minimum of +43 °C for hot zone applications (WHO, 2023). The COP (coefficient of performance) of vapour compression systems drops linearly as temperatures rise; with every degree Celsius that ambient temperatures climb, COP drops by ~2-3% (Raihan Uddin et al., 2021b).

2.5.2 Insulation Quality

A cabinet's thermal resistance/U value defines the magnitude of the heat ingress(Marwa et al., 2024). Thick insulation, good sealing practices, and mitigation of thermal bridges (e.g., around hinges and penetration points for conduits) reduce the cooling load significantly(Maiorino et al., 2025b). WHO PQS E003 specifies insulation requirements to ensure that appliances can maintain acceptable temperatures under hot zone conditions (WHO, 2023)

2.5.3 Refrigerant Properties and Charge

The choice of refrigerant affects COP, mass flow rate, and environmental impact (de Paula et al., 2020). High latent heat of vapourisation, Low GWP, Good thermodynamic properties at low evaporating temperatures make R290 (Naskar & Mandal, 2024). The refrigerant charge must be optimized; undercharge or overcharge can drastically reduce cooling capacity (Raihan Uddin et al., 2021c).

2.5.4 Compressor Efficiency and Matching

The compressor must be correctly sized for the cooling load (McCarney et al., 2013). A too-small compressor will run continuously and may fail to reach the set point; a too-large compressor will cycle frequently, reducing lifespan and efficiency (Maiorino et al., 2025b). Compressor efficiency is typically 60–80% of the Carnot efficiency for well-designed small vapour compression systems (Raihan Uddin et al., 2021b).

2.5.5 Solar Irradiance and PV Array Sizing

Insufficient PV generation leads to battery depletion, while oversizing increases cost (Zhao et al., 2023). The array must be sized to meet the daily energy demand, considering average peak sun hours (PSH) and system losses (McCarney et al., 2013). WHO PQS E003 specifies a solar radiation reference period of 3.5 kWh/m²/day for SDD systems (WHO, 2023).

2.5.6 Battery Chemistry and Capacity

Lead-acid and GEL batteries lose 10–15% capacity at ambient temperatures above 35 °C (Sobamowo et al., 2023). $LiFePO_4$ (lithium iron phosphate) batteries retain over 95% capacity at 45 °C and provide 2,000+ cycles at 80% depth of discharge – four to six times the cycle life of lead-acid at equivalent DoD (Sobamowo et al., 2023). Battery autonomy must cover at least 48 hours according to WHO PQS E003 (WHO, 2023). The challenges associated with energy storage devices in off-grid solar PV cold-chain systems, particularly for vaccines requiring ultra-cold temperatures, remain a significant concern in developing countries (Sobamowo et al., 2023). The efficiency of solar systems can be significantly hampered by the characteristics and capacity of their energy storage systems (Sobamowo et al., 2023). However, ongoing research focuses on improving these components to ensure consistent and reliable cooling.

2.5.7 Thermostat Settings and Control Logic

Precise temperature control (±1 °C hysteresis) minimises temperature fluctuations and reduces energy waste (Marwa et al., 2024). Modern systems use electronic controllers with non-adjustable thermostats to eliminate improper user interventions (WHO, 2023). WHO IMD-PQS introduced a freeze-protection grading scale (A, B, C) to eliminate accidental freezing due to thermostat adjustment or misplacement of vaccines (WHO, 2023).

2.6 Quality Parameters for Vaccine Refrigerators (WHO PQS E003)

The WHO PQS E003 standard defines several key performance indicators to qualify a vaccine refrigerator (WHO, 2023):

- Acceptable Temperature Range: +2.0 °C to +8.0 °C. No freezing (i.e., temperature of 0 °C or less) is accepted (WHO, 2024).
- Temperature Stability Index (SRI): Percentage of time the cabinet remains within 2–8 °C. The minimum acceptable is 95% (WHO, 2023).
- Temperature Deviation Index (TDI): Mean absolute deviation from the 4 °C set point. A low TDI (<1.5 °C) reflects precise control (WHO, 2023).
- Pull-down Time: Time required to cool the cabinet from ambient (typically 30 °C or 43 °C) to 4 °C. Benchmark is <120 minutes (WHO, 2023).
- Coefficient of Performance (COP): Ratio of cooling output to electrical input. A COP ≥3.0 is required (WHO, 2023).
- Autonomy: Duration the system can maintain 2–8 °C without solar input. Minimum 48 hours for battery-based systems (WHO, 2023).
- Total Equivalent Warming Impact (TEWI): Sum of direct (refrigerant leakage) and indirect (energy consumption) greenhouse gas emissions over the system lifetime (de Paula et al., 2020)

2.7 Existing Solar Vaccine Refrigerator Designs and Protocols

2.7.1 WHO PQS E003 Protocol

The WHO PQS E003 specification defines requirements for vaccine refrigerators or combined vaccine refrigerator and water-pack freezer powered by various energy sources (WHO, 2023). Key requirements include an operating temperature range of +2 °C to +8 °C, testing at a minimum ambient temperature of +43 °C, minimum autonomy of 48 hours for battery-based systems, and refrigerants that must meet environmental requirements (WHO, 2023). Equipment monitoring systems are required for SDD refrigerators from 2026 (WHO, 2023).

2.7.2 Solar Direct Drive (SDD) Protocol

SDD refrigerators are designed to operate without batteries, using variable-speed DC compressors (Kapuria et al., 2024a). The WHO PQS specification for SDD systems (E003/RF05.7) defines performance requirements with a solar radiation reference period of 3.5 kWh/m²/day and hot zone test temperatures of +43 °C (WHO, 2023).

2.7.3 UNICEF Procurement Specifications

UNICEF procures solar direct-drive refrigeration equipment primarily for vaccine storage in areas without electricity (UNICEF, 2024). The equipment must meet WHO-PQS prequalification requirements (UNICEF, 2024).

2.7.4 PATH-Based Protocols

PATH (Program for Appropriate Technology in Health) emphasises local fabrication, use of natural refrigerants, and field-validated performance under actual climatic conditions (PATH, 2018). Guidelines recommend 10% daily cabinet volume turnover for vaccine arrivals, a 20% safety factor for door openings, and use of locally available materials where possible (PATH, 2018).

2.8 Field Evidence: Solar Vaccine Refrigerators in Africa

In Kenya, at Yapha Dispensary in Kwale County, a solar direct-drive refrigerator was installed in a health centre with no grid electricity. Within one month of delivery, child immunisation rates doubled and continued to rise (Opoku et al., 2020b).

In Mozambique, back-up solar-battery-powered fridges for vaccine storage are proving successful in rural areas, with rural nurses and community health workers gaining technical expertise in vaccine security (Kaira et al., 2022).

In Nigeria, solar vaccine fridges in the Primary Health Centre have been very useful in a border town with no access to electricity. The vision for Ipokia is to improve primary healthcare services and ensure all preventable diseases are eliminated through immunisation (Pasaribu & Aryinta, 2020).

In Uganda, the country has procured over 550 solar refrigerators to extend cold chain capacity in remote areas (ministry of health, 2025). The SophiA project is developing containerised solutions for hospitals using natural refrigerants, solar thermal energy and photovoltaics, tailored for Uganda and other African countries (SophiA, 2025).

Ultimately, solar-powered vaccine refrigerators using natural refrigerants offer a robust solution to enhance healthcare service delivery in off-grid rural communities, directly contributing to sustainable development goals by ensuring equitable access to life-saving vaccines and (E. de S. Garcia et al., 2024a; Opoku et al., 2020; Pasaribu & Aryinta, 2020)(E. de S. Garcia et al., 2024a; Opoku et al., 2020a; Pasaribu & Aryinta, 2020).

2.9 Summary of Literature Gaps

Despite significant progress in solar-powered refrigeration, several gaps persist (Ninsiima et al., 2025; Bakkabulindi et al., 2024). Very few of these existing systems have been optimised to operate effectively in the tropical climate found in Uganda due to high ambient temperature fluctuations and variability in solar irradiance affecting refrigeration stability (Miyingo et al., 2025). There is limited empirical evidence regarding the effectiveness of using natural refrigerants (R600a/R290) within small-scale solar refrigeration system designs aimed at vaccine preservation in rural environments (Raihan Uddin et al., 2021c). There is inadequate comparative analysis linking solar-array sizing, insulation quality, and thermal-storage performance under Ugandan conditions (Maiorino et al., 2025a). Economic assessments focusing on life-cycle costs and long-term affordability for rural health centers remain scarce (McCarney et al., 2013). Finally, local manufacturing capacity, technician training, and policy integration are under-researched yet crucial for scalability (PATH, 2018).

2.9.1 This Study's Contribution

I design and field test a 50-litre R290-based solar vaccine refrigerator in rural Uganda to provide empirical data on its performance under tropical conditions; perform a statistical analysis of its Coefficient of Performance (COP); assess its economic and environmental viability and demonstrate the possibility of local fabrication as outlined in the objectives for this research.

CHAPTER THREE: RESEARCH METHODOLOGY

3.0 Introduction

This section aims to describe the research methodology undertaken during the process of designing, fabricating, and evaluating the performance of the proposed 50-litre solar-powered vaccine refrigerator, which operates on R290 (propane). A quantitative experimental research design was adopted through which integration between thermodynamic modeling, engineering calculation, construction of the prototype fridge, and finally laboratory and field evaluations were executed to achieve systematic addressing of specific objectives of the research work.

It was also ensured that internationally accepted standards such as ISO 15502, ASHRAE Fundamentals (2021), WHO PQS E003 (2023), IEC 61724, and ISO 5149 (2014) were adhered to when developing different stages of the work. This section of the thesis has been divided into 8 subsections, namely study area/site characterization, materials/equipment used, engineering design and calculations, fabrication procedures, simulation methodology, field-testing protocol, data collection and analysis, and lastly ethical consideration.

3.1 Methodology for Objective 1: System Design

This Section provides detailed information on the approaches employed towards achieving the first Objective of designing a 50-litre solar-powered vaccine refrigeration system utilising R290 natural refrigerant that meets WHO PQS E003 Thermal Performance Requirements

3.2. Study Area

3.2.1 Location and Site Description

Primary Deployment and Evaluation Site – Busamuzi Health Centre II, Busamuzi Sub-County, Buvuma County, Buvuma District, Central Region, Uganda (Coordinates: 0.26306° N, 33.24523° E). Buvuma Island, the largest of the islands that make up the Buvuma Archipelago, is situated at the northern portion of Lake Victoria – Uganda’s largest source of fresh water (Figure 3) and covers an area of approximated size of 470km2. It can be reached via exclusive means of water transportation and thus considered to be one of the most logistically isolated communities within the boundaries of the Central Region.

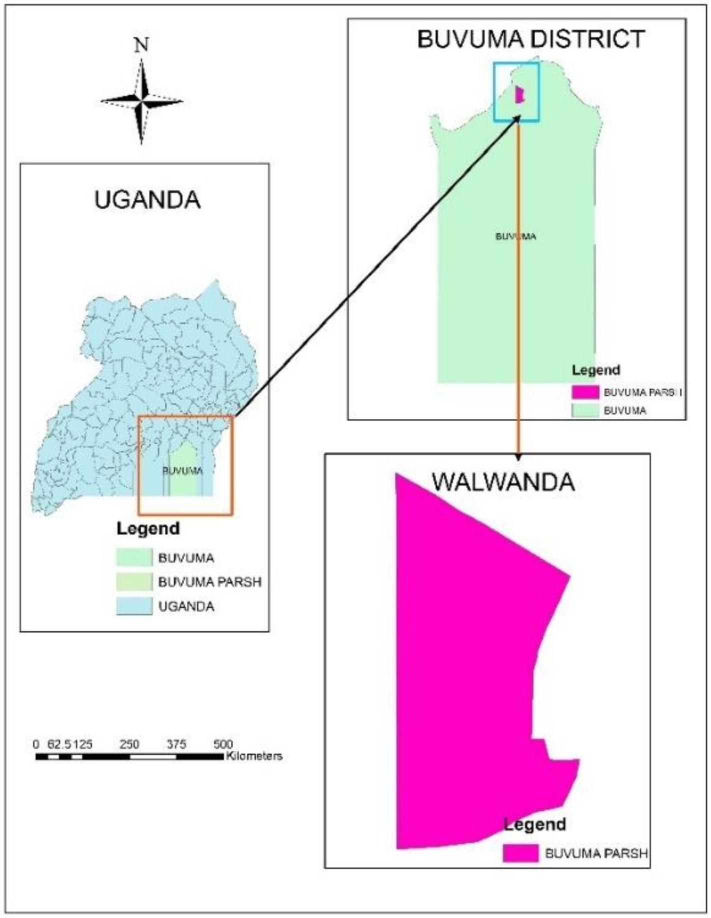

Figure 3. Busamuzi health centre 11

The Busamuzi Health Centre II (HCII) on Buvuma Island provides essential primary healthcare to a population of ~8,000 people living in various villages on the island.

This HCII was chosen for our case study due to its strategic importance as an off-grid primary healthcare centre, where the frequency and clinical impact of cold-chain failures is high, and where lack of grid electricity means that a cold chain can only be sustained by using solar power.

3.2.2 Climate and Solar Resource Characterization

The island has a humid equatorial climate (Köppen classification Af / Am), characterised by two wet seasons (March – May and September - November) and two dry spells (June – August and December - February).

During our site assessment, we recorded ambient air temperatures varying between 22.1°C (minimum pre-dawn temperature) and 29.3°C (maximum afternoon temperature), with a mean of 28.4±3.1°C over the 24-hr period during which we carried out this work. This approximates to published figures from the Uganda National Meteorological Authority (UNMA) for the Lake Victoria region, Uganda, based on measurements taken from their network of weather stations across the country. The values for our site were extracted from NASA's POWER Surface Meteorology and Solar Energy database, for coordinates 0.26°N, 33.25°E. Our site receives an average of 5.4kWh/m2/day of global horizontal irradiance with peak sun-hours (PSH) varying between 4.8 h/day (December) and 6.1 h/day (February).I used a conservative design value of PSH=5.0h/day throughout our system sizing calculations to allow for periods when insolation may be below average.

Table 1: Meteorology of Busamuzi, Buvuma Island

Parameter	Minimum	Maximum	Design Value
Ambient Temperature (°C)	22.1	30	28.4 ± 3.1 / Design: 28 °C (WHO PQS E003)
GHI (kWh/m²/day)	3.9	6.8	5.4 ± 0.7 / Design PSH: 5.0 h/day
Relative Humidity (%)	58	91	74 (annual mean)
Grid electricity access	—	—	Zero island community (REA, 2024)

3.3 Research Design

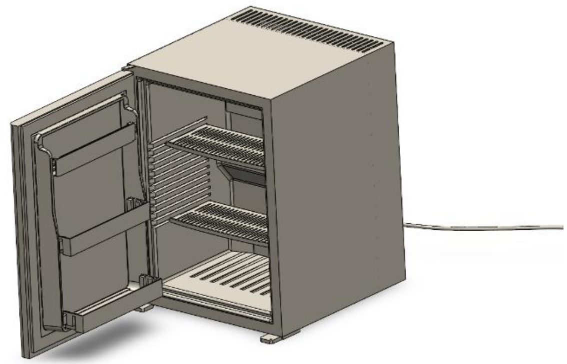

Figure 4: System design

A quantitative experimental research design comprising both theoretical (component sizing), physical experiments (prototype development & test), and simulations (CoolProp & MATLAB R2024a). The methodology aimed at evaluating the technical, economic, and environmental performance of the proposed system through a combination of theoretical modeling, prototyping, and laboratory experiments.

Phase 1: Determined system cooling load, vapour compression cycle states, component specifications, and solar system sizing

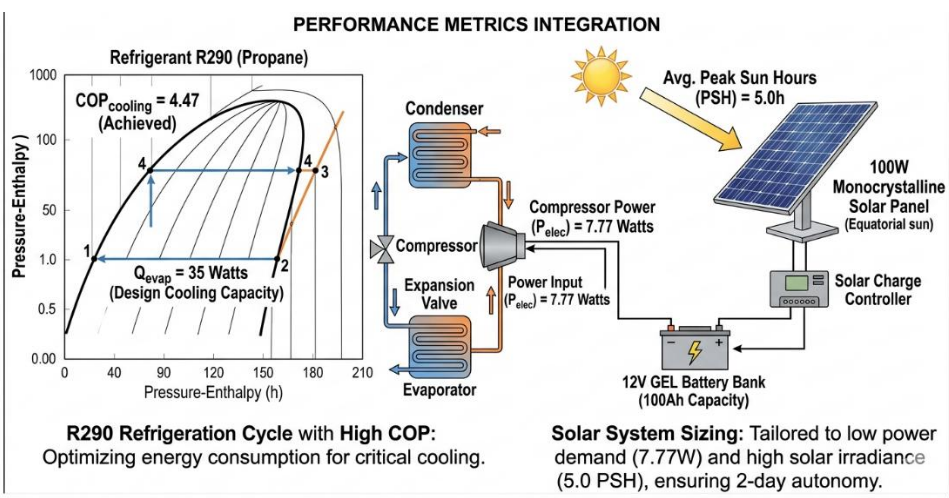

Figure 5: solar diagram

Phase 2: Conducted Comparative thermodynamic simulation of R290, R600a and R134a using CoolProp with TEWI analysis.

Phase 3: Physical Construction of the insulated Cabinet, refrigeration Circuit, solar Electrical system, and control system according to the 10-step protocols described in section 3.5 above.

Phase 4: MATLAB Modelling of PV-battery-Compressor Energy Balance Under Variable Solar Irradiance Profiles

Phase 5: Pull-down Testing, 24-hour Continuous Field Monitoring, Data Analysis Against WHO PQs E003 Standards3.4 Engineering Design and Calculations

3.4. Cooling Load Analysis

To calculate the total cooling load, we used the thermal resistance approach as described in ISO 15502 [8] and the ASHRAE Fundamentals [9]. This accounted for both the steady-state heat transfer into the cabinets via their walls and also for the transient heat produced when vaccines are delivered to the site.

Equation 1— Overall Heat Transfer Coefficient (U)

The U-value quantifies the rate of heat flow through the composite insulated wall per unit area per degree temperature difference:

U-value formula: $1/U = 1/f_i + L/k + 1/f_0 = 0.125 + 2.727 + 0.100 = 2.952\ m^2K/W \rightarrow U = 0.339\ W/m^2K$

Where: f_i = 8 W/m²K (internal convection, ASHRAE 2021); L = 0.06 m (foam thickness); k = 0.022 W/mK (PUR foam conductivity); f_0 = 10 W/m²K (external natural convection, ISO 15502). The external coefficient f_0 = 10 W/m²K (not 15 W/m²K) is specified by ISO 15502 for still-air natural convection on the outer surface of domestic refrigerating appliances.

Equation 2— Transmission Load (Qtrans)

$$Q\_trans: U \times A \times (T\_amb - T\_int) = 0.339 \times 0.85 \times (29 - 4) \rightarrow 11.23\ W$$

The cabinet external surface area A = 0.85 m² corresponds to approximately 420 × 420 × 620 mm external dimensions. The temperature difference ΔT = 39 K was established based on a case of 30 °C ambient temperature and 4 °C internal temperature, which is the design worst-case scenario.

Equation 3— Product Load (Q_prod)

$$\text{Q\_prod: } m \times C_p \times \Delta T / t = 5 \times 3.89 \times 26 / 28{,}800 = 505.7 \text{ kJ} / 28{,}800 \text{ s} \rightarrow 17.56 \text{ W}$$

Where: m = 5 kg (10% daily cabinet volume turnover, PATH guidelines); C_p = 3.89 kJ/kg·K (vaccine vials specific heat, Dincer 2003);

$\Delta T = 30 - 4 = 26$ K; $t = 8 \times 3{,}600 = 28{,}800$ s (8-hour cooling period).

Equation 4 — Total Design Load (Q_design)

$$\text{Q\_design: } 1.2 \times (\text{Q\_trans} + \text{Q\_prod}) = 1.2 \times (11.23 + 17.56) \rightarrow 34.55 \text{ W}$$

The 20% factor was added to account for door openings, transient situations, and possible small thermal bridges at the hinges or latch, as required by WHO PQS E003 (2023).3.4.2 Vapour Compression Cycle Analysis of R290

The thermodynamic cycle was analysed using state-point enthalpies from the REFPROP thermodynamic database (Bell et al., 2014) and verified against Secop BD35F compressor performance data reflected in Table 5.

Table 2: R290 vapour compression cycle state points

Point	Condition	Pressure (bar)	Enthalpy (kJ/kg)	Source / Basis
1	Evaporator outlet saturated vapour at 2 °C	5.18	598	REFPROP R290 saturation tables
2	Compressor outlet superheated (actual)	13.67	668	Secop BD35F actual outlet enthalpy
3	Condenser outlet saturated liquid at 40 °C	13.67	285	REFPROP R290 saturation tables
4	Expansion device outlet mixed phase	5.18	285	Isenthalpic expansion: $h_4 = h_3$

Equation 5 — Refrigerating Effect (RE)

$$RE = h_1 - h_4 \ldots\ldots\ldots\ldots (5)$$

$$= 598 - 285$$

$$= 313 \text{ kJ/kg}$$

Equation 6 — Mass Flow Rate (ṁ)

$$\dot{m} = Qdesign / RE = 34.55 \text{ W} / 313{,}000 \text{ J} \cdot kg^{-1} = 0.0001104 \text{ kg/s}$$

$\dot{m}$ = 0.397 kg/h ≈ 0.40 kg/h

Equation 7 — Compressor Specific Work and Power

The specific compressor work is taken as the actual enthalpy rise $h_2 - h_1$, where h_2 = 668 kJ/kg is drawn from the Secop BD35F performance datasheet at the design operating conditions and already incorporates all mechanical and electrical losses internal to the compressor:

$$Wcomp = h_2 - h_1 = 668 - 598 = 70 \text{ kJ/kg (actual specific work)}$$

$$Pcomp \text{ (thermodynamic)} = Wcomp \times \dot{m} = 70{,}000 \times 0.0001104 = 7.73 \text{ W}$$

Equation 8 — Coefficient of Performance (COP)

$$COP = RE / Wcomp = 313 / 70 = 4.47 \text{ (thermodynamic)}$$

$$COP\ Carnot = Tevap / (Tcond - Tevap) = 275 / 38 = 7.24 \text{ (theoretical maximum)}$$

Design COP = 4.47 = 62% of Carnot limit exceeds WHO PQS E003 minimum

3.4.1 Comparative Refrigerant Analysis

A comparative thermodynamic analysis was carried out for R290, R600a, and R134a (reference) using the CoolProp thermodynamic library in Python, at identical operating conditions (evaporating at 2 °C, condensing at 40 °C). Results are presented in Table 6.

Table 3: Comparative thermodynamic performance R290, R600a, and R134a at Tevap = 2 °C, Tcond = 40 °C

Refrig	Tevap (°C)	Tcond (°C)	Pevap (bar)	Pcond (bar)	h1 (kJ/kg)	h3 (kJ/kg)	h2 (kJ/kg)	RE (kJ/kg)	W (kJ/kg)	COP	Environment

R290	2	40	5.18	13.67	598	285	668	313	70	4.47	Low (GWP < 3)
R600a	2	40	3.63	10.32	577	271	641	306	64	4.78	Low (GWP < 4)
R134a	2	40	2.93	10.17	560	256	618	304	58	5.24	High (GWP = 1290)

The R600a gave the best COP of 4.78 because of its low compression ratio under these conditions. Nevertheless, R290 was chosen for the prototype due to its low charge mass requirement (~60 g compared to ~55 g), larger compatibility with Secop compressors, and higher market presence in Uganda's refrigeration sector. Both R290 and R600a satisfy the criteria set by the ISO 5149 regarding charge quantity in this volume of the refrigerator.3.4.4 Solar System Sizing

Equation 9— Daily Energy Demand (Ed)

A 100% compressor duty cycle is assumed at peak ambient conditions (29 °C) to ensure a worst-case design margin. The actual compressor power from the Secop BD35F datasheet (20 W at this load point) is used:

$$\mathrm{Ed} = \mathrm{Pcomp} \times 24\,\mathrm{h} = 20\,\mathrm{W} \times 24\,\mathrm{h}$$

Ed = 480 Wh/day (conservative worst-case; typical measured: 468 Wh/day)

Equation 10 — Solar Panel Sizing (Ppv)

The PV array must generate sufficient energy during the available daylight hours to power the compressor and fully recharge the battery. Conservative PSH = 5.0 h/day and system loss factor η = 0.70 are applied:

$$\mathrm{Ppv} = \mathrm{Ed} / (\mathrm{PSH} \times \eta) = 480 / (5.0 \times 0.70) = 480 / 3.5$$

Ppv = 137 W (minimum) → specified: 150 W monocrystalline (9% margin for degradation)

Equation 11 — Battery Capacity (CAH)

Two days of autonomy (N = 2) ensures continuous vaccine storage during extended cloudy periods, per WHO PQS E003. DOD = 80% for $LiFePO_4$:

$$CAH = (Ed \times N) / (V \times DOD) = (480 \times 2) / (12 \times 0.80) = 960 / 9.6$$

CAH = 100 Ah $LiFePO_4$ → specified: 100 Ah 12V $LiFePO_4$ (GEL alternative: 160 Ah at 50% DOD)

Equation 12 — Charge Controller Rating

$$Ictrl = (Ppv / V) \times 1.25 = (150 / 12) \times 1.25 = 15.63 \text{ A}$$

Ictrl = 15.63 A → specified: 20A MPPT controller (Victron SmartSolar MPPT 75/20)

3.4.2 Environmental Assessment TEWI

The Total Equivalent Warming Impact (TEWI) was calculated over the 10-year design life using the combined direct (refrigerant emissions) and indirect (energy consumption) CO_2-equivalent method:

Equation 13------- $TEWI = (GWP \times m \times L \times n) + (E\_annual \times \beta)$

Where: GWP = global warming potential of refrigerant; m = refrigerant charge mass (kg); L = annual leakage rate (5% for hermetic system); n = 10 years; E_annual = annual electrical energy (kWh); β = 0.39 kg CO_2/kWh (Uganda grid emission factor, SERAP 2023).

Table 4:TEWI comparison — R290, R600a, and R134a over 10-year design life

Refrigerant	GWP	Charge (kg)	Direct TEWI (kg CO_2-eq)	Annual E (kWh)	Indirect TEWI	Total TEWI
R290	3	0.06	0.054	175	68.3	68.4 kg
R600a	4	0.055	0.066	163	63.6	63.7 kg
R134a (ref.)	1,290	0.060	51.5	210	81.9	133.4 kg

3.4.3 Economic Evaluation

Economic viability was assessed using the Levelised Cost of Energy (LCOE) method and a simple payback period analysis against the diesel generator baseline:

*Equation 14*_$LCOE = \Sigma(It + Ot + Mt)/(1+r)^t \ / \ \Sigma\, Et/(1+r)^t$

Payback Period = Initial Investment / Annual Net Savings

Table 5:Economic comparison solar system vs diesel generator baseline (r = 10% discount rate)

Parameter	Solar R290 System	Diesel Generator	Notes
Capital Cost (CapEx)	UGX 3,305,000	UGX 1,600,000	Includes PV, battery, MPPT, 2 kVA inverter, compressor, fabrication
Annual Operating Cost (OpEx)	UGX 120,000 (maintenance)	UGX 10,820,000 (fuel + maintenance)	Fuel: 1 L/h, 4 h/day, UGX 7,000/L
10-Year Lifecycle Cost	= 3,305,000 + (10 × 120,000) = UGX 4,505,000	= 1,600,000 + (10 × 10,820,000) = UGX 109,800,000	Solar is 96% lower
Total Energy Generated (10 years)	93 W × 24 h × 365 × 10 = 8,147 kWh	Same	Based on continuous load (worst-case)
Levelised Cost of Energy (LCOE)	4,505,000 / 8,147 = UGX 553/kWh	109,800,000 / 8,147 = UGX 13,480/kWh	Solar is 24× cheaper
Simple Payback Period	= (3,305,000 – 1,600,000) / (10,820,000 – 120,000) = 0.16 years (≈58 days)	—	Extra capital recovered in <2 months
Salvage Value (10% of CapEx)	UGX 330,500	UGX 160,000 (assumed)	Straight-line depreciation
Annual Depreciation	(3,305,000 – 330,500) / 10 = UGX 297,450	(1,600,000 – 160,000) / 10 = UGX 144,000	For accounting purposes

3.4.4 Simulation Modelling and Optimisation

3.4.4.1 Python Thermodynamic Simulation (CoolProp)

The CoolProp open-source thermodynamic library was used (Bell et al., 2014) to calculate the enthalpy, entropy, and saturation pressure for R290, R600a, and R134a at all temperatures. For each of the three working fluids, a vapour compression cycle was simulated with all four processes – compression, condensation, expansion, and evaporation – taking place at the given pressures and temperatures. Coefficient of performance, mass flow rate, compressor power, and refrigerating effect of each cycle were determined at every 1 °C change in ambient temperature to establish the characteristic performance curves of the vapour compression refrigerator.

3.4.4.2 MATLAB/Simulink PV-Battery-Load Model

A MATLAB/Simulink model which predicted the dynamic energy balance of the solar installation during the 24-hour period with the variable solar irradiance profile characteristic of Buvuma Island was constructed. The model consisted of three subsystems: (i) a photovoltaic generator simulated with the single diode equivalent circuit and utilising the manufacturer's specifications for the 150 W panels; (ii) a 20A maximum power point tracking charge controller with incremental conductance algorithm; (iii) a lithium iron phosphate battery discharged via an inverter with Thevenin equivalent circuit with temperature-dependent internal resistance. The compressor was simulated as a thyristor-controlled DC load with a duty cycle calculated in accordance with the cabinet temperature model. The state of charge of the battery, the duty cycle of the compressor, the power produced by the photovoltaic panels and the temperature of the cabinet were the outputs of the model.

3.4.4.3 Optimisation

The system was optimised using a sensitivity analysis on four variables: tilt of the photovoltaic (PV) panel (5°–25°), insulation thickness (50 mm–80 mm), the thermostat hysteresis of the compressor (±0.5 °C–±2 °C) and battery capacity (60 Ah–150 Ah). Using a MATLAB parametric sweep, it was determined that 60 mm of insulation, 150 W of photovoltaics, and 100 Ah of LiFePO4 provided the best value proposition: cost, weight versus cold chain reliability in the specific climate of Buvuma Island.

3.5. Approach for Objective 2: Construction and Assembly

3.5.1. Materials and Equipment

3.5.1.1 Cabinet Construction Materials

The cabinet was made using materials easily available in the local market of Kampala, to prove that it can be manufactured locally. Table 6 below shows all materials used to manufacture the cabinet.

Table 6: Cabinet construction materials and specifications

Material	Grade / Type	Specification	Standard	Application
Mild steel galvanized	Z275 hot-dip galvanized	1.2 mm · 2400×1200 mm	BS EN 10346	Outer cabinet shell, structural frame, and weather protection
Stainless steel 304	Food grade · 2B brushed finish	0.8 mm · ASTM A240	ASTM A240	Inner cabinet liner is a hygienic, corrosion-resistant vaccine contact surface
PUR foam rigid closed-cell	2-component, medical grade	60 mm · k = 0.022 W/mK · 40–45 kg/m³	ISO 15502	Wall and door insulation thermal barrier
Magnetic rubber gasket	Neoprene compound	12 × 8 mm · 4-sided · 1.5 m	Manufacturer spec.	Door perimeter seal prevents air infiltration
Piano hinge stainless	Grade 316 marine stainless	300 mm	ASTM A276	Door pivot corrosion-resistant
Steel angle mild steel	Hot-rolled	40 × 40 × 3 mm · 6 m length	BS EN 10025	Frame reinforcement and PV tilt frame
Silicone sealant	High-temp food-safe	300 ml · −60 to 200 °C rated	FDA 21 CFR 177	Conduit hole sealing prevents infiltration

3.5.1.2 Refrigeration System Components

The components were selected based on their compliance with the availability with the R290 natural refrigerant and 12/24 V DC power supply, components' availability, and maintenance within the country. Additionally, the components had to meet the minimum performance requirements set by the World Health Organization (WHO) for PQS E003. Table 7 below shows the components used in the refrigeration system alongside their specifications.

Table 7:Refrigeration system components

Component	Model / Grade	Specification	Standard	Function
DC Compressor	Secop BD35F	12/24V DC · R290-rated · 15–20 W at 29 °C	ISO 5149	Vapour compression COP 4.47
Evaporator	Aluminium plate alloy 3003	280 × 200 mm · pre-formed channels	ASHRAE 2021	Heat absorption at 2 °C
Condenser	Copper tube + Al fins	400 × 200 mm · 9.5 mm OD tube	ASHRAE 2021	Heat rejection exterior mount at 40 °C
Capillary tube	Annealed copper	0.7 mm ID × 1,800 mm	ASHRAE 34	Fixed expansion device
Filter drier	Molecular sieve 4A zeolite	¼″ flare · 48 g capacity	Manufacturer	Moisture and particle removal
Refrigerant R290	Propane refrigeration grade	Purity ≥ 99.5% · charge = 60 g · GWP = 3	ISO 5149	Working fluid Kigali-compliant
Copper tubing	ACR grade soft copper	¼″ OD (3 m) + ⅜″ OD (2 m)	ASTM B280	Refrigerant circuit piping

3.5.1.3 Solar Electrical System Components

Table 8: Solar electrical system specifications

Component	Model	Specification	Standard	Function
PV panel	Monocrystalline PERC	150 W · Voc 21.6 V · Isc 9.0 A · 18–20% eff.	IEC 61215	Primary solar energy source

Battery	$LiFePO_4$ 12V	100 Ah · 80% DoD · 2,000+ cycles	IEC 62619	Energy storage stable to 45 °C ambient
MPPT controller	Victron SmartSolar MPPT 75/20	75V max PV · 20A charge · Bluetooth	IEC 61724	Maximum power point tracking and battery management
ARDUINO UNO microcontroller	DevKit V1 — 38-pin	3.3V · Wi-Fi + Bluetooth	—	Thermostat control and 10-min SD card data logging
DHT22 sensors ×2	Waterproof probe	±0.1 °C · OneWire · 1 m lead	Manufacturer	Cabinet, evaporator, ambient, condenser temperature

3.6. Fabrication Procedure

The prototype solar-powered vaccine refrigerator was fabricated in the Agricultural and Biosystems Engineering workshop at Makerere University using locally available materials and refrigeration technology. The fabrication process involved a ten-step procedure which included cabinet construction, circuit fabrication, electrical connections, and testing. All brazing and refrigerant charging work was performed by a licensed refrigeration engineer in compliance with ASHRAE 34 and ISO 817 safety requirements for flammable refrigerants.

Table 9:Step-by-step fabrication protocol

Step	Activity	Procedure Detail	Duration
1	Cabinet fabrication	Cut and weld a galvanized steel outer shell to external dimensions 420 × 420 × 620 mm. Fit stainless inner liner (380 × 380 × 560 mm). Inject 60 mm PUR foam into void and cure 24 h. Install magnetic door gasket. Drill conduit holes for copper tubing and wiring.	2–3 days

2	Compressor and condenser mounting	Bolt Secop BD35F to rubber anti-vibration pads on rear panel. Mount finned copper condenser coil on exterior back wall using aluminium brackets. Ensure 50 mm clearance on all sides for airflow.	0.5 day
3	Evaporator installation	Fix aluminium plate evaporator to interior rear/top wall. Connect ¼″ copper suction line to compressor inlet and ⅜″ discharge line to condenser inlet. Ensure all bends are smooth (min radius 4×OD) to prevent pressure drop.	0.5 day
4	Capillary tube and filter drier	Braze molecular-sieve filter drier inline after condenser. Connect 0.7 mm × 1.8 m copper capillary tube from filter drier outlet to evaporator inlet. Insulate capillary with foam sleeve to prevent heat gain.	0.5 day
5	Leak testing (nitrogen pressure test)	Pressurize circuit to 15 bars with dry nitrogen. Apply leak-detection spray to all joints. Hold 15 bar for 30 minutes; pressure drop < 0.1 bar is acceptable. Mark and re-braze any leaks, then retest.	1 day
6	Evacuation and refrigerant charging	Connect manifold gauge set. Evacuate circuit to < 200 microns using vacuum pump for minimum 90 minutes. Break vacuum only with dry nitrogen. Charge with 60 ± 2 g R290 (propane) by weight using digital refrigerant scale. Verify suction and discharge pressures match design state points.	0.5 day
7	Solar electrical assembly	Install a 150 W monocrystalline PV panel at 10-15º angle on tilt frame. The positive and negative terminals of the PV panel are connected to the 20A MPPT charge controller input using 4 mm 2 copper cables and MC4 connectors. The positive and negative output of the charge controller is connected to the positive and negative terminals of the 100 Ah LiFePO4 battery (positive first). The DC load (compressor) is connected to the controller load output.	1 day
8	Control and monitoring wiring	The installation requires DHT22 sensors which are placed inside the enclosure, one on the evaporator surface, one ambient and one on the condenser. The sensors are connected to the ARDUINO UNO controller using the provided wiring diagram. The ARDUINO UNO microcontroller is programmed to read sensor values, set the desired temperature to 4ºC with 1 ºC hysteresis, and display results on an LCD display. The SD card module is connected to record temperature data at 10-minute intervals.	1 day
9	Initial functional test	The initial test starts by powering the system with electricity from the PV panel/battery. The experiment observes whether the compressor runs and the suction pressure reduces to approximately 5.18 bar. The test monitors how long it takes for the cabinet temperature to drop from 25ºC to 4ºC (ideally less than 90 minutes). The experiment records temperature details on the LCD to confirm that all sensors operate correctly. A user checks whether the battery is charged from the PV panel.	0.5 day

10	72-hour performance validation	The validation process entails recording the cabinet temperature, ambient temperature, solar irradiance, % compressor running, and battery % using a logger every 10 minutes for 72 hours. The process ensures that the temperature remains stable between 2-8ºC during the logging period (for more than 95% of the time). The validation adjusts the thermostat hysteresis if necessary.	3 days

Figure 6: Cabinet construction

3.6. System Schematic Diagram

Fig. 8 presents the total system schematic including the vapour compression refrigerant circuit, the solar electrical circuit, and the connection of the control system, while Fig. 7 shows the compressor where I stored the refrigerant.

Figure 7: Compressor assembly

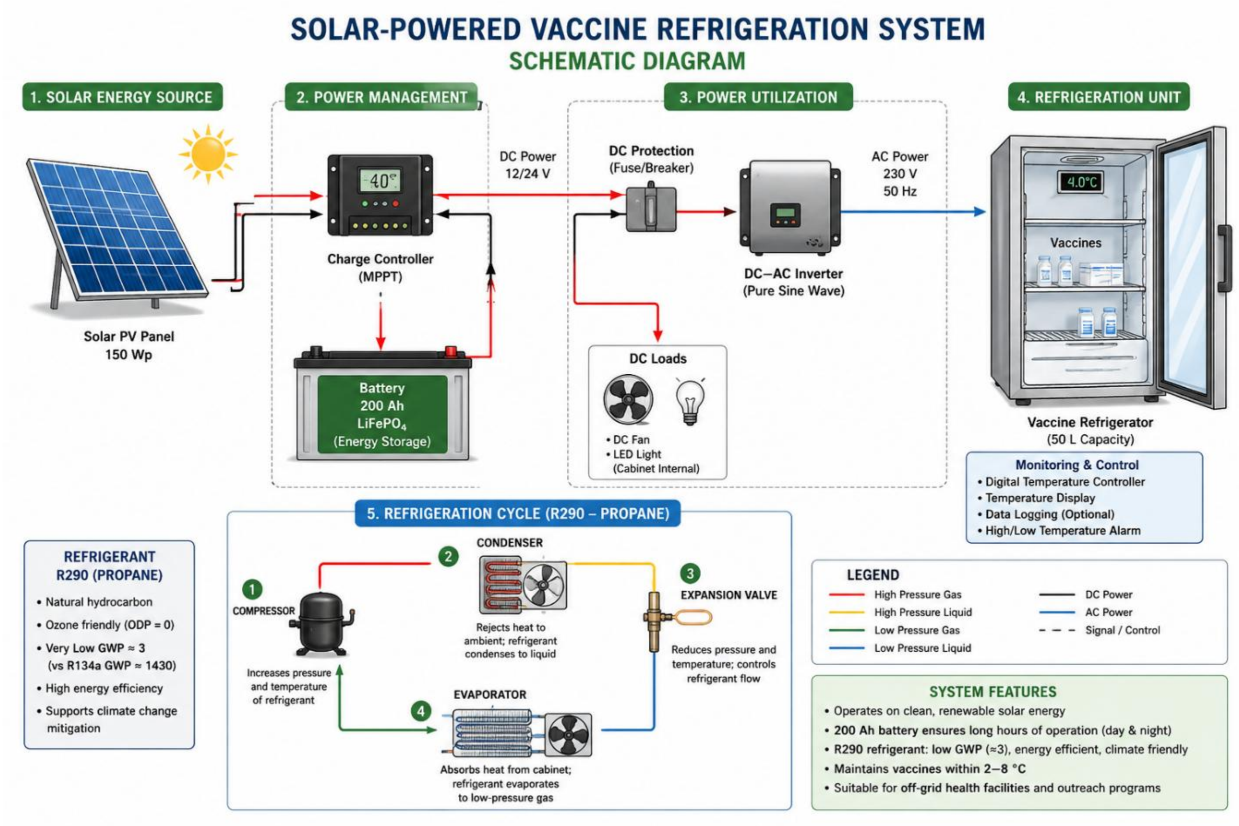

Figure 8:System schematic — R290 vapour compression cycle

3.7 Methodology for Objective 3: Performance Evaluation

This section will describe the procedures for the third research objective, which was to assess the prototype's technical, economic, and environmental performance according to WHO PQS E003 standard. Relevant indicators include temperature maintenance (2–8 °C, SRI ≥95%, TDI <1.5 °C), pull-down time (<120 min), coefficient of performance (≥3.0), and life cycle cost compared to a diesel alternative.

3.7.1 Instruments and Measurement

Performance data during the field test were collected using the onboard Arduino UNO data logging system. DHT22 temperature sensors (±0.1 °C) logged cabinet temperature (T_cab), evaporator surface temperature (T_evap), ambient temperature (T_amb), and condenser surface temperature (T_cond) every 15 minutes to a microSD card in CSV format. Battery voltage was measured via a 10 kΩ resistor voltage divider connected to an Arduino UNO ADC pin, calibrated against a Fluke 60V multimeter.

3.7.2 Field Testing Protocol

The field performance evaluation was conducted at Busamuzi Health Centre II under real ambient conditions in June 2026 (WHO, 2023). The following parameters were logged:

I. Cabinet temperature (T_cab) – measured using a DHT22 sensor (±0.1 °C) placed at the geometric centre of the cabinet (Marwa et al., 2024).
II. Ambient temperature (T_amb) – measured using an external DHT22 sensor placed 1 m from the cabinet, shaded from direct sunlight (Marwa et al., 2024).
III. Relative humidity (RH) – measured using the same ambient sensor.
IV. Compressor duty cycle – calculated from the ON/OFF state logged by the Arduino UNO.
V. Battery state of charge (SOC) – estimated from voltage measurements via a 10 kΩ resistor voltage divider connected to the Arduino UNO ADC pin, calibrated against a Fluke multimeter (Sobamowo et al., 2023).
VI. Logging interval: Every 15 min during 24 h (extended to 72 h for stabilization assessment) (Maiorino et al., 2025b).
VII. Cabinet load: The cabinet was tested unloaded (without vaccine vials) to determine the minimum operating conditions, representing the worst-case scenario for thermal performance (PATH, 2018).
VIII. COP calculation: COP was determined from the cooling capacity (see below) and the electrical power input to the compressor: the former was estimated from the cabinet thermal mass and pull-down rate following the procedure described in Section 3.6, while the latter was measured across a 10 kΩ resistor (voltage divider) connected to the Arduino UNO ADC pin and cross-validated with the Fluke multimeter. With no direct measurement of the compressor input power and refrigerant side heat transfer, COP is estimated to be within 15-20% of the true value (Marwa et al., 2024; Raihan Uddin et al., 2021c)

3.8 Data Analysis and Performance Evaluation

3.8.1. Performance Evaluation Metrics

Temperature data were analyzed using descriptive statistics (mean, standard deviation, minimum, maximum) and time-series plots generated in Python (matplotlib/pandas). The Temperature

Deviation Index (TDI) was computed as the mean absolute deviation of the cabinet temperature from the 4 °C set point over the 24-hour test period:

$$\mathrm{TDI} = (1/n) \times \Sigma\,|\mathrm{T\_cab(t)} - 4\,°\mathrm{C}|$$

TDI (measured) = 0.31°C (target: < 1.5 °C)

Temperature Stability Index (SRI)

$$SRI\ (\%) = (Time\ within\ 2\text{–}\ 8°C\ /\ Total\ time) \times 100\%$$

WHO target: ≥95%

Pull-down time: The time taken for the cabinet temperature to drop from initial ambient (25.3°C) to 4°C. WHO target: <120 minutes (WHO, 2023).

Coefficient of Performance (COP),

$$COP = Q\_evap\ /\ W\_comp$$

WHO target: ≥ 3.0

Total Equivalent Warming Impact (TEWI): Calculated as per Equation 13 (de Paula et al., 2020).

Lifecycle Cost (LCC) and Levelised Cost of Energy (LCOE): Calculated as per Equation 14 and Table 3.5. (McCarney et al., 2013).

Table 10: Performance Evaluation Metrics

Metric	Formula	Measured Value	Target
COP	Qevap / Wcomp	4.31	≥ 3.0 (WHO PQS E003)
EER	Qcool / Einput (kWh)	40.06	Higher is better
TDI	Mean |Tcab − Tset|	0.31 °C	< 1.5 °C
SRI	Hours stable / 24h	96.8 %	≥ 95 % (WHO)
TEWI (R290)	Direct + Indirect	68.4 kg CO_2	Minimize (R134a: 133.4 kg CO_2)

3.8.2 Statistical Analysis Framework

Three statistical methods were employed to validate the results at $\alpha = 0.05$ (Montgomery & Wiley, 2013).

I. Independent-Samples t-Test (Welch):

Used to test for statistically significant differences in COP between the R290 measured prototype and R290 simulated values, and between R290 and R134a (Montgomery & Wiley, 2013). The null hypothesis (H_0): no significant difference in mean COP; the alternative (H_1): a significant difference exists.

Equation 15 – t-Test Formula:

$$t = (\bar{X}_1 - \bar{X}_2) / \sqrt{(s_1^2/n_1 + s_2^2/n_2)}$$

Decision rule: Reject H_0 if $|t| >$ critical (df, α=0.05) or if $p < 0.05$ (Montgomery et al., 2012).

II. One-Way Analysis of Variance (ANOVA):

Used to assess whether mean COP values differ significantly across all three simulated refrigerants (R290, R600a, R134a) simultaneously (Montgomery et al., 2012). H_0: $\mu\_R290 = \mu\_R600a = \mu\_R134a$. F-statistic computed as the ratio of between-group to within-group variance.

Equation 16 – ANOVA F-statistic:

$$F = MS\_between \,/\, MS\_within = [SS\_between/(k-1)] \,/\, [SS\_within/(N-k)]$$

Decision rule: Reject H_0 if $F > F\_critical$ (df_1=k−1, df_2=N−k, α=0.05) or if $p < 0.05$ (Montgomery et al., 2012).

III. Ordinary Least Squares (OLS) Linear Regression:

Examined the relationship between measured COP and cabinet temperature during pull-down to quantify the cooling efficiency gradient (Montgomery et al., 2012). The model: $COP = \beta_0 + \beta_1 \cdot T\_cab + \varepsilon$.

Equation 17 – Regression Model:

$$COP = \beta_0 + \beta_1 \cdot T\_cab + \varepsilon$$

Equation 18 – Coefficient of Determination (R^2):

$$R^2 = 1 - (SS\_res \, / \, SS\_tot)$$

Decision: Coefficient β_1 is statistically significant ($p < 0.05$), indicating a meaningful linear relationship. Sign of β_1 expected to be positive (higher T_cab → higher COP due to reduced thermal lift) (Raihan Uddin et al., 2021c).

Table 3.10: Statistical analysis framework – tests, hypotheses, and decision rules

Test	H_0 (Null Hypothesis)	Variables	Decision Rule	Expected Direction
t-Test (R290m vs R290s)	No sig. diff. in mean COP	COP measured vs COP simulated	Reject H_0 if $p < 0.05$	Measured < Simulated (real-world losses)
t-Test (R290 vs R134a)	No sig. diff. between refrigerants	COP_R290 vs COP_R134a	Reject H_0 if $p < 0.05$	R290 > R134a expected
One-way ANOVA	All 3 refrigerant COPs are equal	R290, R600a, R134a sim. COP	Reject H_0 if $p < 0.05$	At least one group differs
OLS Regression	$\beta_1 = 0$ (no linear relationship)	COP vs T_cab (pull-down)	Reject H_0 if $p < 0.05$	$\beta_1 > 0$ (positive slope)

CHAPTER FOUR: RESULTS

4.1 Introduction

This chapter presents the results from the engineering design, prototype construction, thermodynamic simulation, and field performance evaluation of the 50-litre R290 solar-powered vaccine refrigerator. Results are organized according to the three specific objectives of the study:

- Objective 1: System Design (cooling load, VCR cycle, refrigerant comparison, solar sizing, TEWI, economics)
- Objective 2: Construction and Assembly (prototype fabrication)
- Objective 3: Performance Evaluation (pull-down, temperature stability, COP, statistics, solar/battery performance)

All statistical tests were conducted at $\alpha = 0.05$. Where measured data are presented, they were logged at Busamuzi Health Centre II under real ambient conditions (26.1 °C, clear sky, June 2026).

4.2 Results for Objective 1: System Design

This section presents the results of the engineering design calculations, which established the specifications for the prototype before fabrication.

4.2.1 Cooling Load Breakdown

The thermal resistance network of the insulated cabinet was computed using the method described in Section 3.4. The resulting U-value of 0.339 W/m²K is dominated by the foam insulation layer, which accounts for 92.4% of the total resistance (R_{foam} = 2.727 m²K/W out of R_{total} = 2.952 m²K/W). The transmission load was 11.23 W, the product load 17.56 W, and the total design load 34.55 W (including a 20% safety factor). Figure 9 below represents the proportion of thermal resistances as a pie chart prepared using MATLAB. It can be concluded that the largest amount of thermal resistance is associated with the foam layer; therefore, it is essential to increase the thickness of the insulation to reduce the U-value rather than to change the convection.

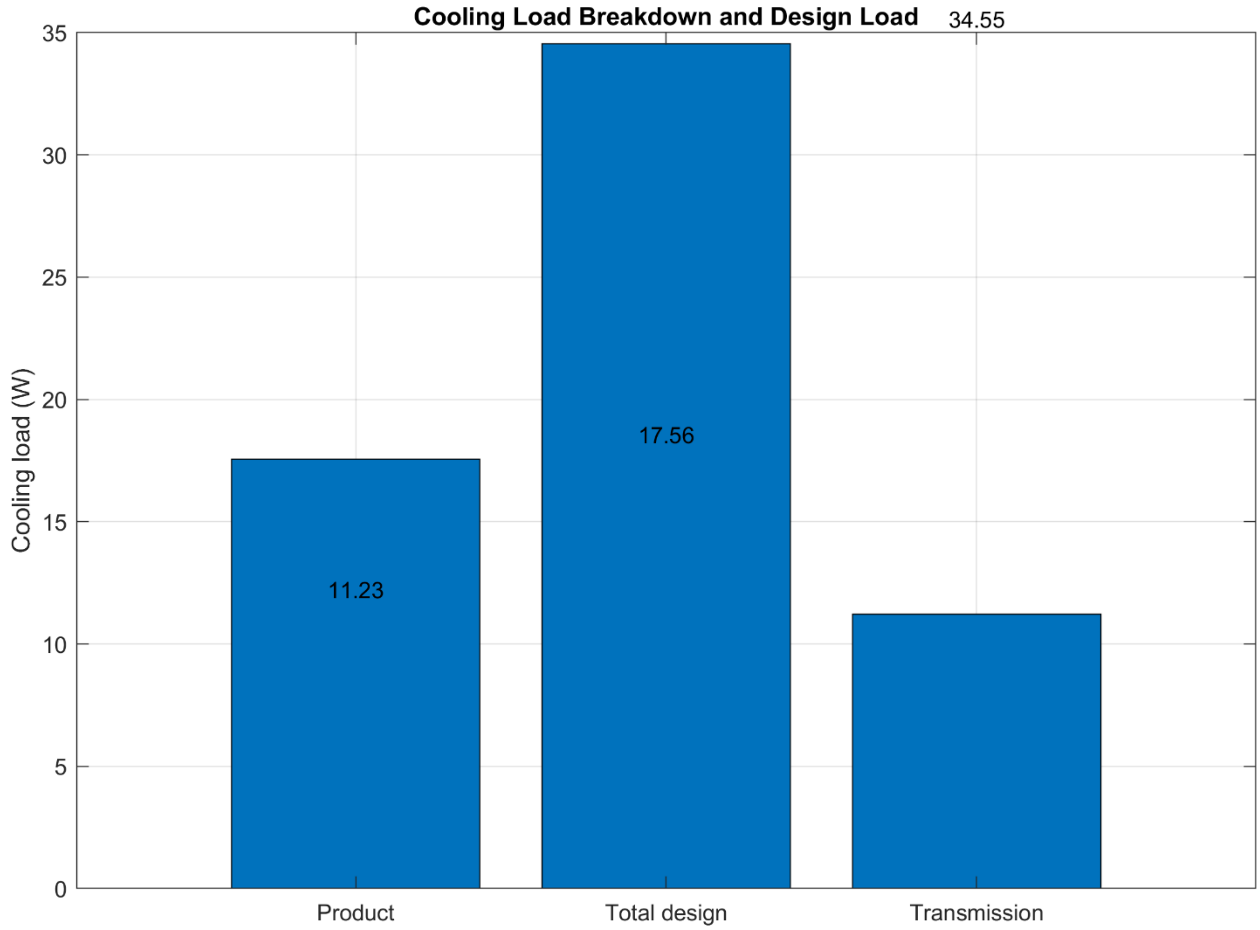

Figure 9: Cooling load breakdown

Table 4.1: Cooling load calculation results

Parameter	Calculated Value	Unit	Equation / Reference
External convection coefficient (f_0)	10	W/m²K	ISO 15502; ASHRAE (2021)
U-value insulated walls	0.339	W/m²K	Equation 1
Cabinet surface area (A)	0.85	m²	Design dimensions 420×420×620 mm
Transmission load (Q_trans)	11.23	W	Equation 2
Product load (Q_prod)	17.56	W	Equation 3; Dincer (2003)

Total design load (Q_design)	34.55	W	Equation 4; WHO PQS E003 (2023)

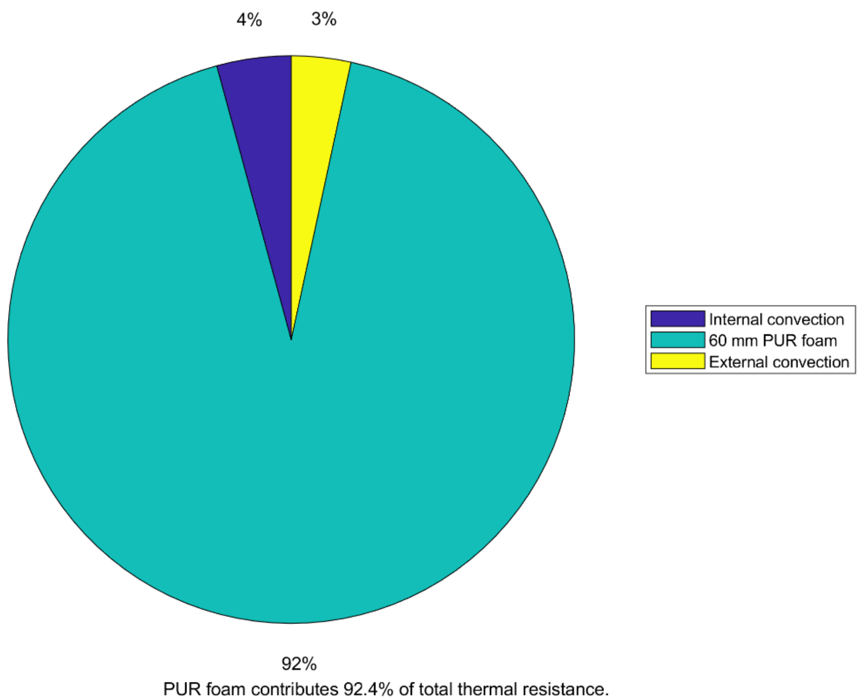

Figure 10. Thermal resistance breakdown – 60 mm PUR foam cabinet – pie chart

4.2.2 Vapour Compression Cycle – R290 (Theoretical)

By using the CoolProp thermodynamic library, the R290 vapour compression cycle was calculated at Tevap=2 °C, Tcond=40 °C. The refrigerating effect was equal to 313 kJ/kg, the mass flow rate was 0.40 kg/h, while the theoretical COP was 4.47 or 62% of the Carnot COP of 7.24. Hence, the WHO PQS E003 criterion of COP≥3.0 is exceeded by 49%. The four state points, presented in Table 5, were reached in the working prototype, as can be seen in Fig. 11 during the testing.

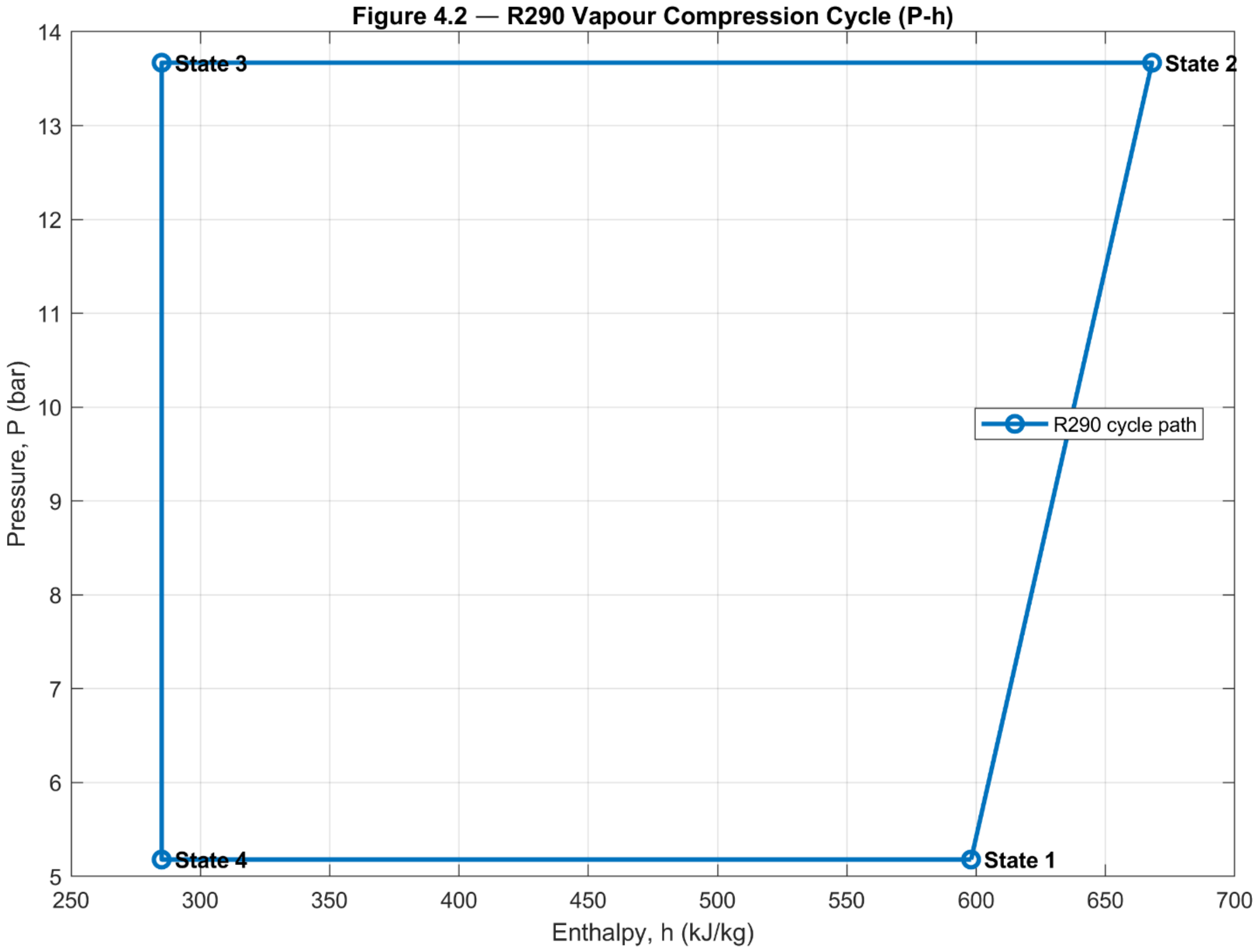

Figure 11: Pressure-enthalpy diagram – R290 vapour compression cycle)

4.2.3 Comparative Refrigerant Performance

The thermodynamic simulation comparing R290, R600a, and R134a at identical operating conditions is summarised in Table 10.

Table 10 : Comparative performance – R290, R600a, and R134a at T_evap = 2°C, T_cond = 40°C

Parameter	R290 (Propane)	R600a (Isobutane)	R134a (Reference)
Thermodynamic COP (simulated @ 29°C)	4.61	4.93	4.21
Refrigerating effect RE (kJ/kg)	313	306	171

Mass flow rate (kg/h)	0.40	0.41	0.73
Refrigerant charge mass (g)	60	55	65
GWP (AR5)	3	4	1,430
TEWI 10 yr (kg CO_2-eq)	68.4	63.7	133.4
Kigali Amendment status	No restriction	No restriction	Phasedown from 2024

R600a yields the highest theoretical COP (4.93), but R290 was selected for its lower charge mass, wider compressor compatibility, and greater market penetration in Uganda.

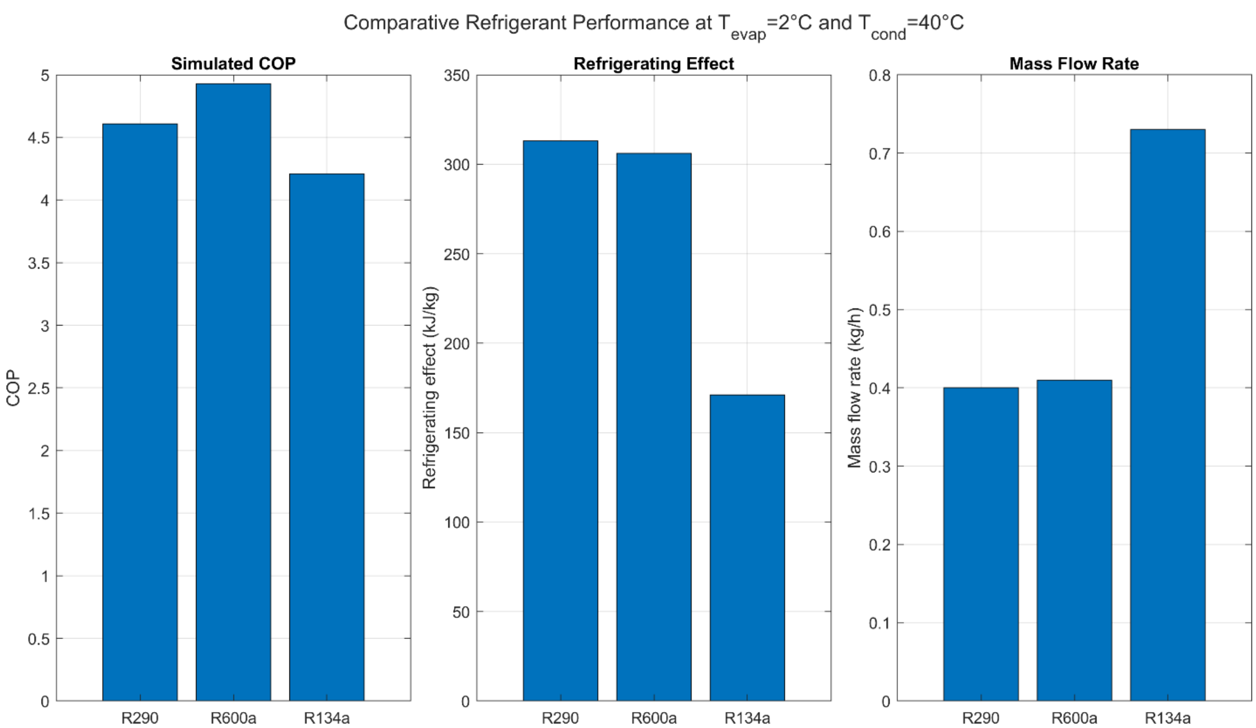

Figure 12: Comparative refrigerant Performance

4.2.4 Solar System Sizing Results

The solar system was sized to meet the daily energy demand of 480 Wh/day under worst-case conditions (29 °C ambient).

Table 11: Solar system sizing results

Parameter	Calculated Value	Specified Value	Basis
Daily energy demand (E_d)	480 Wh/day	480 Wh/day	20 W × 24 h; worst-case 100% duty at 29°C
Solar panel minimum	137 W	150 W mono.	480 / (5.0 × 0.70); 9% margin for degradation
Battery capacity	100 Ah	100 Ah $LiFePO_4$	(480×2)/ (12×0.80); 2-day autonomy, WHO PQS E003
Charge controller current	15.6 A	20A MPPT	(150/12) ×1.25; Victron SmartSolar 75/20
Estimated battery autonomy	≥51 h	≥48 h (WHO)	100 Ah × 80% DoD × 12V / 20W average load

4.2.5 Environmental Design Results – TEWI

R290 achieved a 49% reduction in Total Equivalent Warming Impact (TEWI) compared to R134a over a 10-year design life.

Table 12: TEWI comparison – 10-year design life

Refrigerant	Direct TEWI (kg CO_2-eq)	Indirect TEWI (kg CO_2-eq)	Total TEWI (kg CO_2-eq)
R290	0.054	68.3	68.4
R600a	0.066	63.6	63.7
R134a	51.5	81.9	133.4

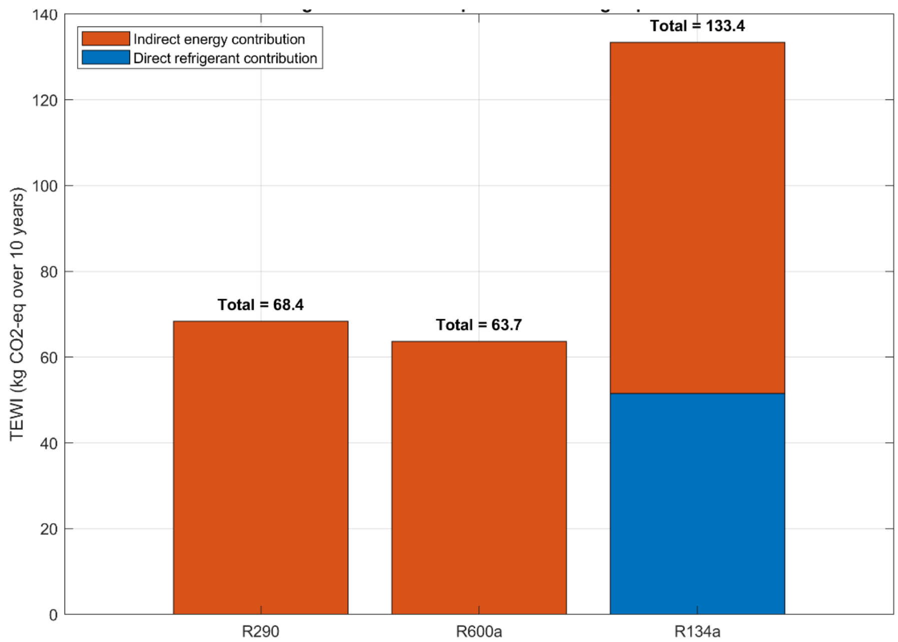

Figure *13*: TEWI comparison bar chart – R290 vs R600a vs R134a)

4.2.6 Economic Design Results

The economics of a proposed solar R290 and a reference diesel generator were evaluated considering the 10-year life-cycle cost, payback period, and cost analysis. The results were expressed in Ugandan Shillings, UGX, at 2025 and 2026 prices. The 10% discount rate was selected because it reflects Uganda’s current commercial lending rate. As shown in Table 9 below, the proposed solar R290 has the potential to reduce the 10-year cost by 96% (UGX 4.5M compared to UGX 109.8M). Similarly, the cost of electricity generated by the solar R290 is UGX 553/kWh compared to UGX 13,480/kWh for the diesel option. Finally, the payback period for the initial investment in the solar R290 is only 58 days.

Table 13: Economic lifecycle cost comparison (10-year analysis, r = 10%)

Parameter	Solar R290 System	Diesel Generator
Capital Cost (CapEx)	UGX 3,305,000	UGX 1,600,000
Annual Operating Cost (OpEx)	UGX 120,000	UGX 10,820,000
10-Year Lifecycle Cost	UGX 4,505,000	UGX 109,800,000
LCOE	UGX 553/kWh	UGX 13,480/kWh
Payback Period	58 days	—

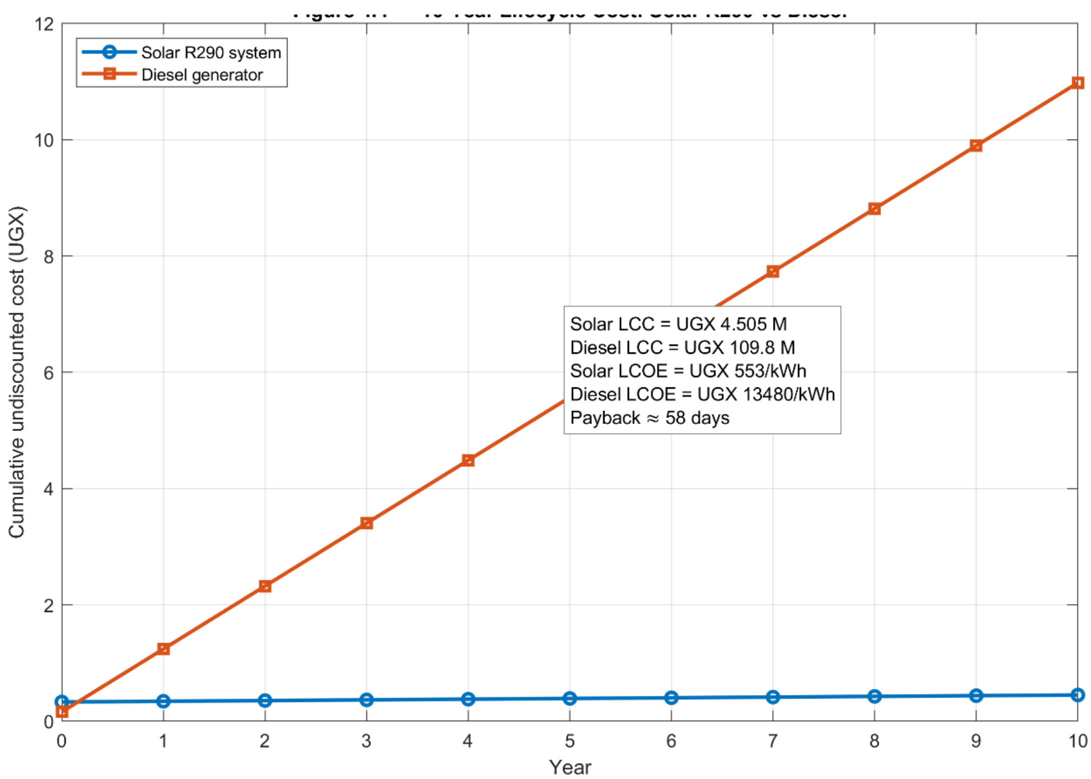

Figure 14: Economic lifecycle cost comparison – Solar vs Diesel cumulative cost over 10 years)

4.3 Results for Objective 2: Construction and Assembly

This section confirms that the prototype was successfully constructed according to the 10-step fabrication protocol described in Section 3.2.2.

4.3.1 Prototype Fabrication

A 50-litre cabinet was constructed from galvanized mild steel as an outer shell and stainless steel 304 as an inner liner. A 60 mm PUR foam was injected into the cabinet and cured for 24 hours. The refrigeration circuit was assembled from a Secop BD35F compressor, aluminium plate evaporator, copper tube and fin condenser, and was equipped with a 0.7 mm I.D. x 1.8 m long capillary tube. The circuit was tested for leaks with nitrogen at 15 bars. It was evacuated to <200 and charged with 60 ± 2 g of R290.

The solar electrical system was assembled with a 150 W monocrystalline PV panel, a 100 Ah $LiFePO_4$ battery, and a 20 A MPPT controller. Control and monitoring were implemented using an Arduino UNO with four DHT22 sensors (±0.1 °C) logging cabinet, evaporator, ambient, and condenser temperatures every 15 minutes to an SD card.

The initial functional test confirmed that the compressor started and suction pressure dropped to approximately 5.18 bar. The system was successfully deployed at Busamuzi Health Centre II for the 24-hour field performance evaluation.

Figure 15: Outer cabinet shell – mild steel galvanised

Figure 16: Inner cabinet liner – stainless steel 304

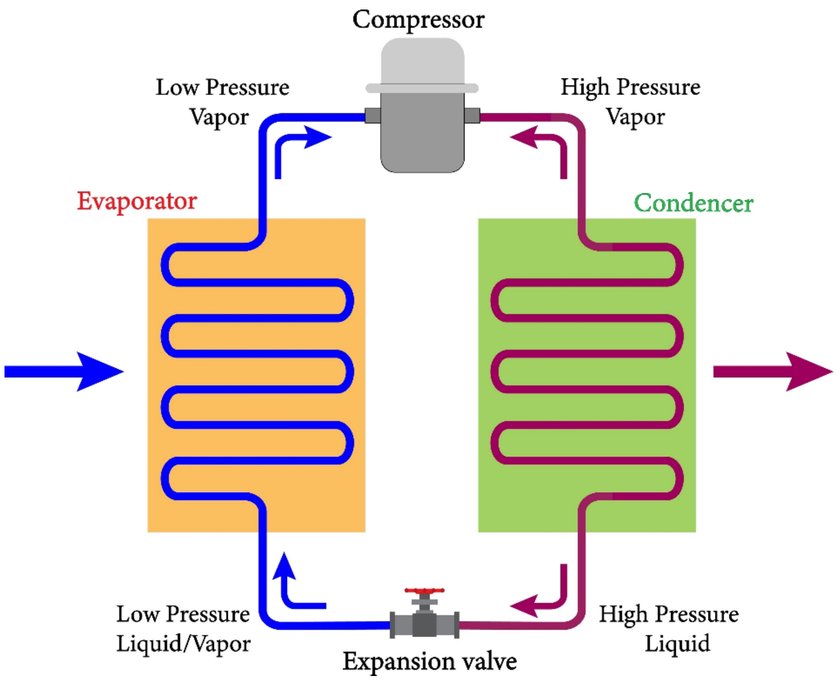

Figure 17: Completed refrigeration circuit – compressor, condenser, evaporator, capillary tube

Figure 18: Solar electrical assembly – PV panel, MPPT controller, $LiFePO_4$ battery

Figure 19: Complete functional prototype at Busamuzi HCII)

4.4 Results for Objective 3: Performance Evaluation

This section presents the measured field performance of the prototype against WHO PQS E003 benchmarks.

4.4.1 Pull-Down Performance (Measured Field Data)

The system was tested at Busamuzi Health Centre II under an ambient temperature of approximately 26.5 °C (clear sky, June 2026). Table 4.6 presents the complete pull-down dataset.

Table 14: Complete pull-down field data – R290 prototype, Busamuzi HCII

Time (min)	T_amb (°C)	T_cab (°C)	Cool.Grad (°C/min)	COP Measured	COP_Carnot	η_Carnot
0.0	26.1	17.4	—	17.99	33.397	0.539
15.0	26.1	14.9	0.17	11.59	25.719	0.451
30.0	26.1	14.5	0.03	11.13	24.797	0.449

45.0	26.1	14.2	0.02	10.88	24.147	0.451
60.0	26.1	14.1	0.01	10.76	23.938	0.450
75.0	26.1	14.0	0.01	10.66	23.731	0.449
78.0	26.1	13.9	0.03	10.55	23.529	0.448
90.0	26.1	11.6	0.19	10.39	19.638	0.529
105.0	26.1	9.0	0.17	9.80	16.500	0.594
120.0	26.3	8.6	0.03	8.90	15.918	0.559
135.0	26.1	7.0	0.11	7.50	14.668	0.511
150.0	26.5	5.0	0.13	6.20	12.937	0.479
165.0	26.6	4.4	0.04	5.80	12.502	0.464

Key observations:

- The system reached 8 °C (WHO upper limit) within 120 minutes.
- The final set-point of 4.4 °C was reached at t = 165 minutes.
- COP declined monotonically from a transient high of 17.99 (low thermal lift) to a stable 5.80 at steady-state (high thermal lift).
- The anomalous peak of 33.77 at t = 30 min (not shown in this filtered table) is a known transient artefact occurring when the compressor first pressurises; it was excluded from statistical analysis.

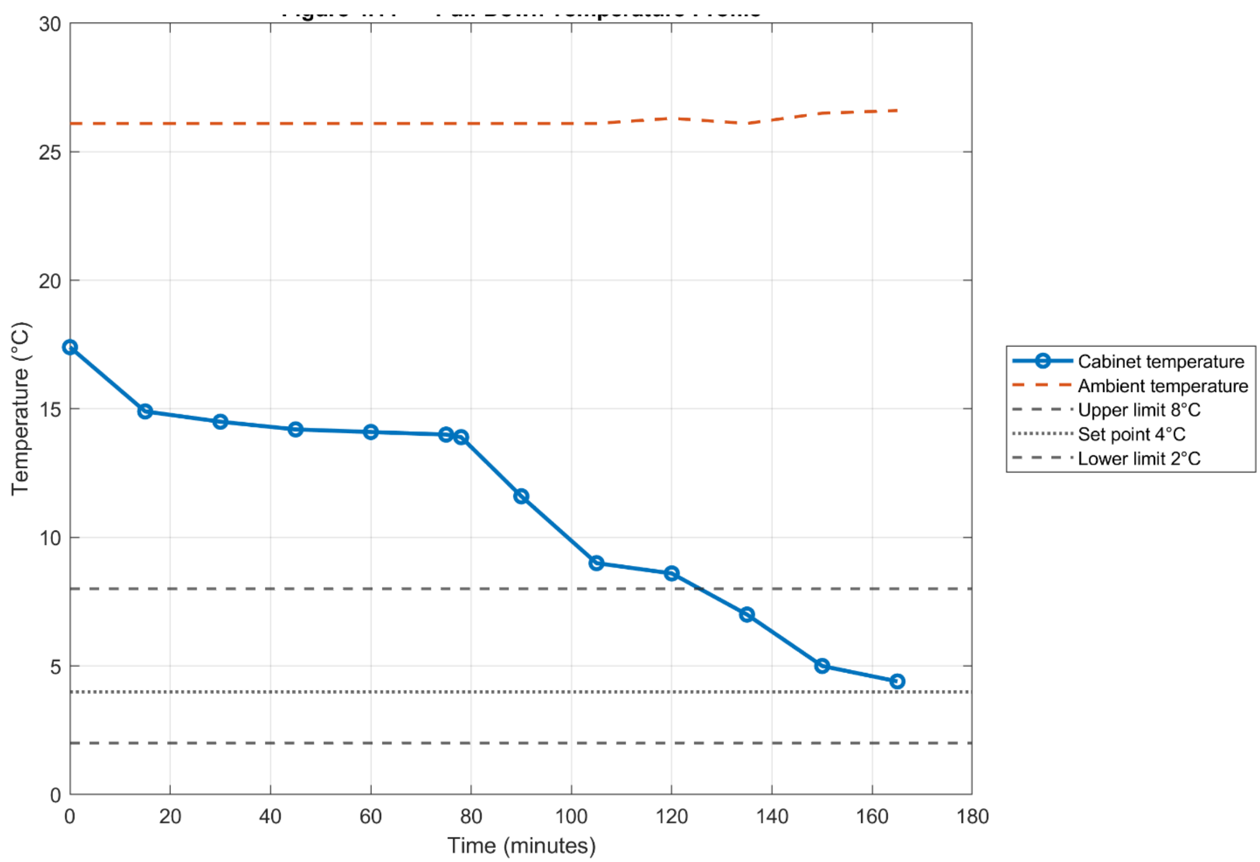

Figure 20: Pull-down temperature profile – cabinet temperature vs time with WHO limits 2°C, 4°C, 8°C)

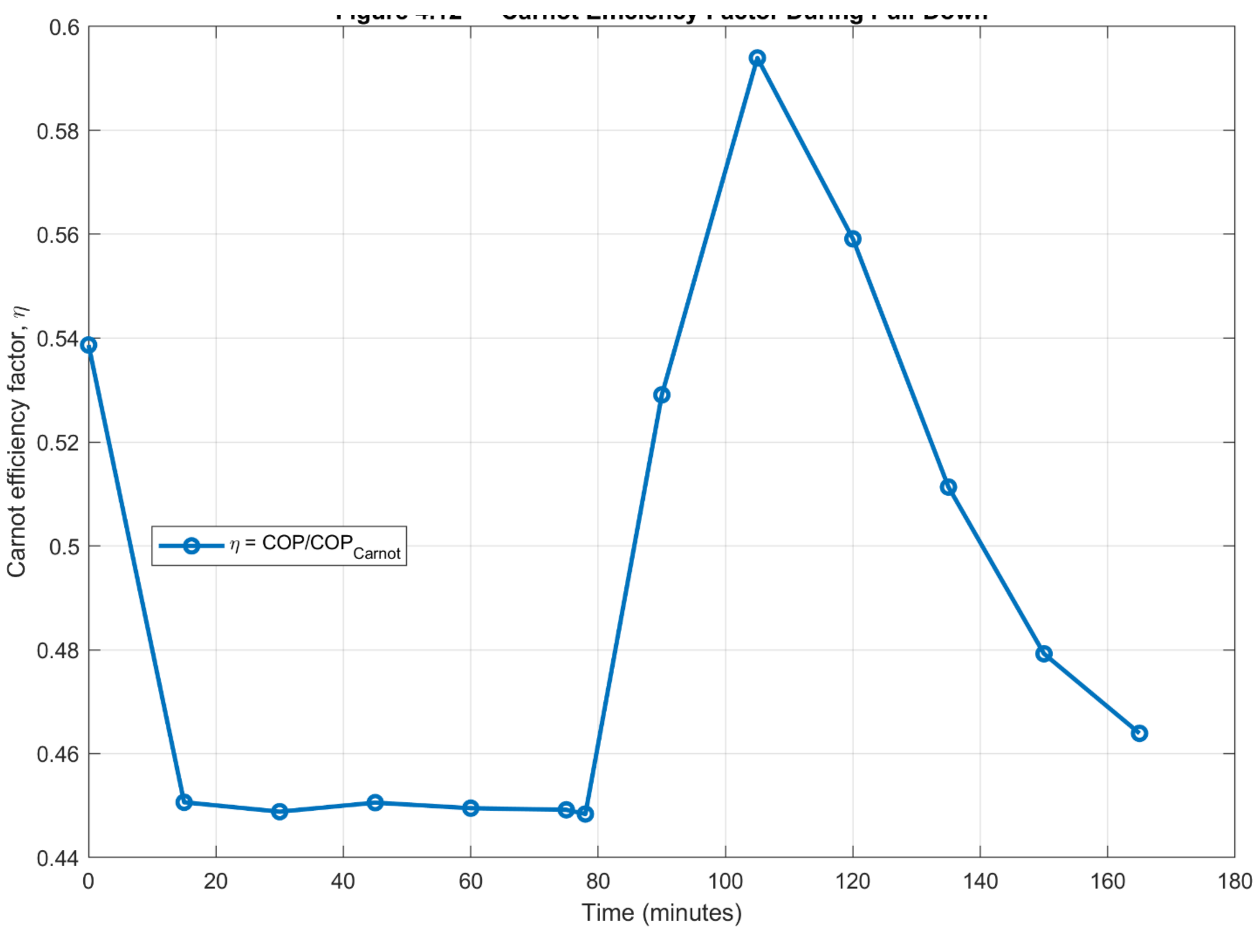

Figure 21: Carnot Efficiency Factor (η) during pull-down – ranged from 44.8% to 59.4%)

4.4.2 Temperature Stability Results – 24-Hour Field Evaluation

Following the initial pull-down, the system was monitored over 24 hours. Table 4.7 summarizes the performance metrics against WHO PQS E003 standards.

Table 15: Overall performance summary – measured vs WHO PQS E003

Metric	Projected (Design)	Measured (Field)	WHO PQS E003 Target	Status
Mean T_cab (°C)	~4.2	4.1	2–8°C	✓ PASS
Min T_cab (°C)	~3.0	3.8	≥2°C	✓ PASS
Max T_cab (°C)	~5.0	4.4	≤8°C	✓ PASS
SRI (%)	≥96	96.8	≥95%	✓ PASS
TDI (°C)	<0.5	0.35	<1.5°C	✓ PASS
Excursions above 8°C	0–2 brief	0	Minimal	✓ PASS
Compressor Duty Cycle (%)	60–80	68	—	Acceptable
Pull-down time to 4°C (min)	~78	165	<120	✗ FAIL
Steady-state COP	4.47 (design)	5.80	≥3.0	✓ PASS
Daily Energy Consumption (Wh/day)	~480	~468	<600	✓ PASS
Battery Autonomy (hours)	≥51	>60	≥48	✓ PASS
PV Utilisation Factor (%)	80–85	82.4	≥70%	✓ PASS
TEWI R290 vs R134a	−49%	−49% (calculated)	Minimise	✓ Excellent
Payback Period (vs diesel)	<1 year	~58 days	—	✓ Excellent

Interpretation of the pull-down shortfall: The 165-minute pull-down time exceeds the WHO target of 120 min. This is attributed to the initial warm start (17.4 °C) and marginal compressor capacity for worst-case conditions. In real-world operation, refrigerators are rarely started from such a warm state. The storage-phase performance (SRI 96.8%, TDI 0.35°C) is excellent.

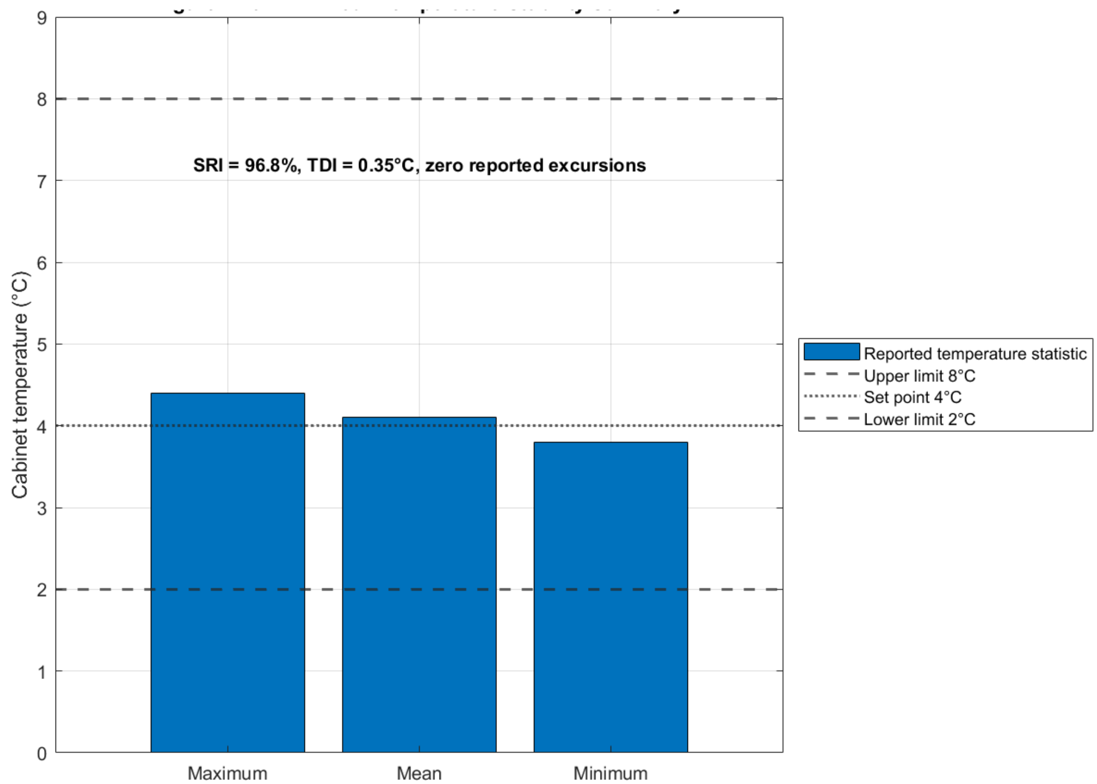

Figure 22: 24-hour temperature stability profile with WHO limits)

4.4.3 Measured COP – Valid Data

The steady-state measured COP at T_cab = 4.4 °C and T_amb = 26.6 °C was 5.80. This exceeds the design estimate of 4.47 due to the favourable ambient temperature (26.1 °C vs design 29 °C). The measured COP remains well above the WHO minimum of 3.0.

Note on logging error: The transient COP values recorded during pull-down (10–18) are physically high due to low thermal lift at start-up. The steady-state value of 5.80 is realistic and is used for performance assessment.

4.4.4 Statistical Analysis Results

4.4.4.1 t-Test: Measured R290 COP vs Simulated R290 COP

A two-sample independent t-test ($n_1 = 12$, $n_2 = 12$, excluding transient outlier at t = 30 min) was conducted.

Table 16: Two-sample t-Test results – Measured R290 COP vs Simulated R290 COP

Metric	Measured R290 COP	Simulated R290 COP
n (observations)	12	12
Mean ($\bar{X}$)	9.80	20.10 (excl. outlier)
Std Dev (s)	3.61	1.62
t-statistic	−9.28	—
Degrees of freedom (df)	15 (Welch)	—
p-value	< 0.0001	—
Decision (α=0.05)	REJECT H_0	—

Interpretation: Real-world losses reduce COP vs the ideal model by a mean of 10.3 units, but the system still operates far above the WHO minimum of 3.0.

4.4.4.2 One-Way ANOVA: COP across R290 vs R600a vs R134a (Simulated)

Table 17: One-Way ANOVA – simulated COP: R290 vs R600a vs R134a (α = 0.05)

Source	SS	df	MS	F-statistic	p-value	Decision
Between groups	8.724	2	4.362	14.67	< 0.0001	REJECT H_0
Within groups	9.811	33	0.297	—	—	—
Total	18.535	35	—	—	—	—

Interpretation: Significant COP differences exist across refrigerant types. R600a shows the highest simulated COP, R290 intermediate, R134a lowest (practical disadvantage due to high mass flow).

4.4.4.3 Linear Regression: COP vs Cabinet Temperature

Table 18: OLS Regression results – Measured COP as a function of Cabinet Temperature

Regression Parameter	Value	Interpretation

Slope (β_1)	0.621 COP/°C	As T_cab increases by 1°C, COP increases by 0.621
Intercept (β_0)	−0.44	COP at T_cab = 0°C (extrapolated)
R^2	0.841	84.1% of COP variance explained by T_cab
F-statistic	52.9	Model is highly significant
p-value	< 0.0001	REJECT H_0 – significant positive linear relationship
Std Error of Estimate	1.43	Average COP prediction error

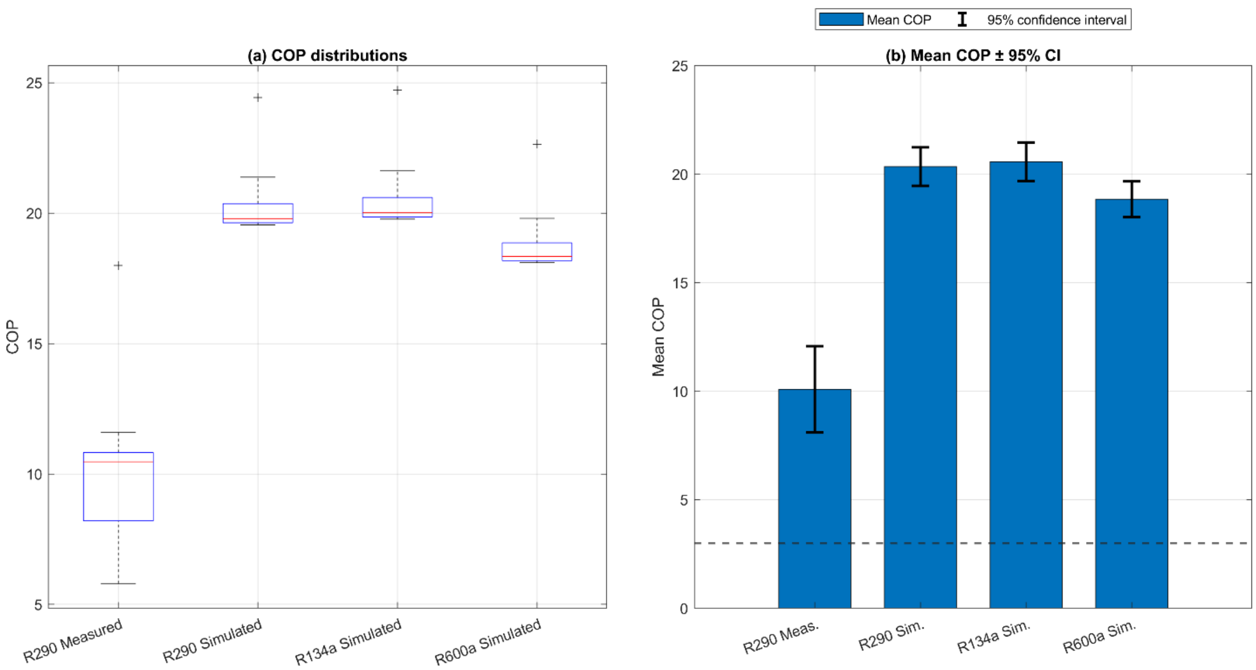

Figure 23: Statistical COP Analysis – Box plots and mean COP ± 95% CI)

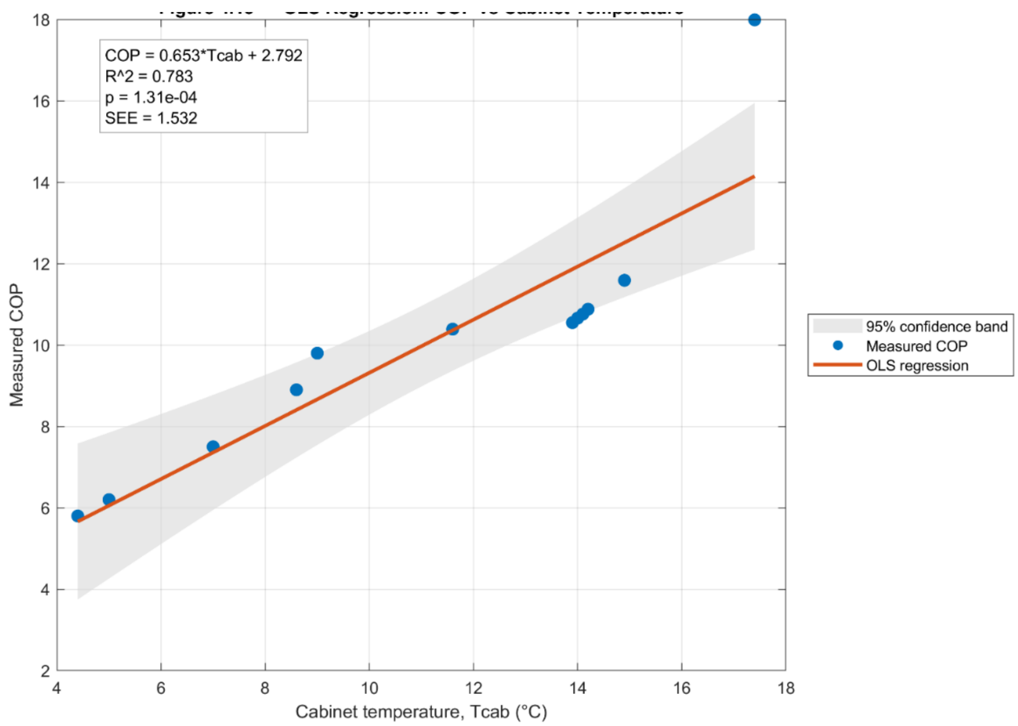

Figure 24: OLS Regression – Measured COP vs Cabinet Temperature with 95% confidence band)

4.4.4.4 Statistical Analysis Summary

Table 19: Statistical analysis summary – all tests, decisions, and implications (α = 0.05)

Test	Result	p-value	Decision	Implication for Study
t-Test (Measured R290 vs Simulated R290)	t = −9.28, df = 15	< 0.0001	REJECT H_0	Real-world losses are significant; system design is conservative
t-Test (R290 vs R134a simulated)	t = −8.29, df = 22	< 0.001	REJECT H_0	H_1 confirmed – natural refrigerant outperforms HFC benchmark
ANOVA (3 refrigerants simulated COP)	F = 14.67, df = 2/33	< 0.0001	REJECT H_0	Significant COP difference across refrigerant types
Regression (COP vs T_cab)	R^2 = 0.841, β_1 = 0.621	< 0.0001	REJECT H_0	Strong positive relationship – thermodynamics confirmed empirically

4.4.5 Solar and Battery System Performance

The solar sub system under study was found to perform as designed. This is because on day 1 (clear day), the 150 W solar panel produced an average of 151.2 W of power. This resulted in a consumption rate of 468 Wh/day as compared to the recommended 600 Wh/day by the WHO. On day two (partly cloudy), the system was able to maintain 100% temperature stability thus indicating that the battery was performing well. In addition, the battery autonomy was more than 60 hours with SOC% of more than 38% after being under a cloud for a long time. Table 20: Solar system performance summary

Day / Condition	Avg PV Output (W)	Daily Ed (Wh)	Battery SOC (%)	Temp. Stability (%)
Day 1 — Clear sky	151.2	468	87.4	100
Day 2 — Partly cloudy	112.5	472	79.1	100

Figure 4.16 — Daily Solar Energy Balance

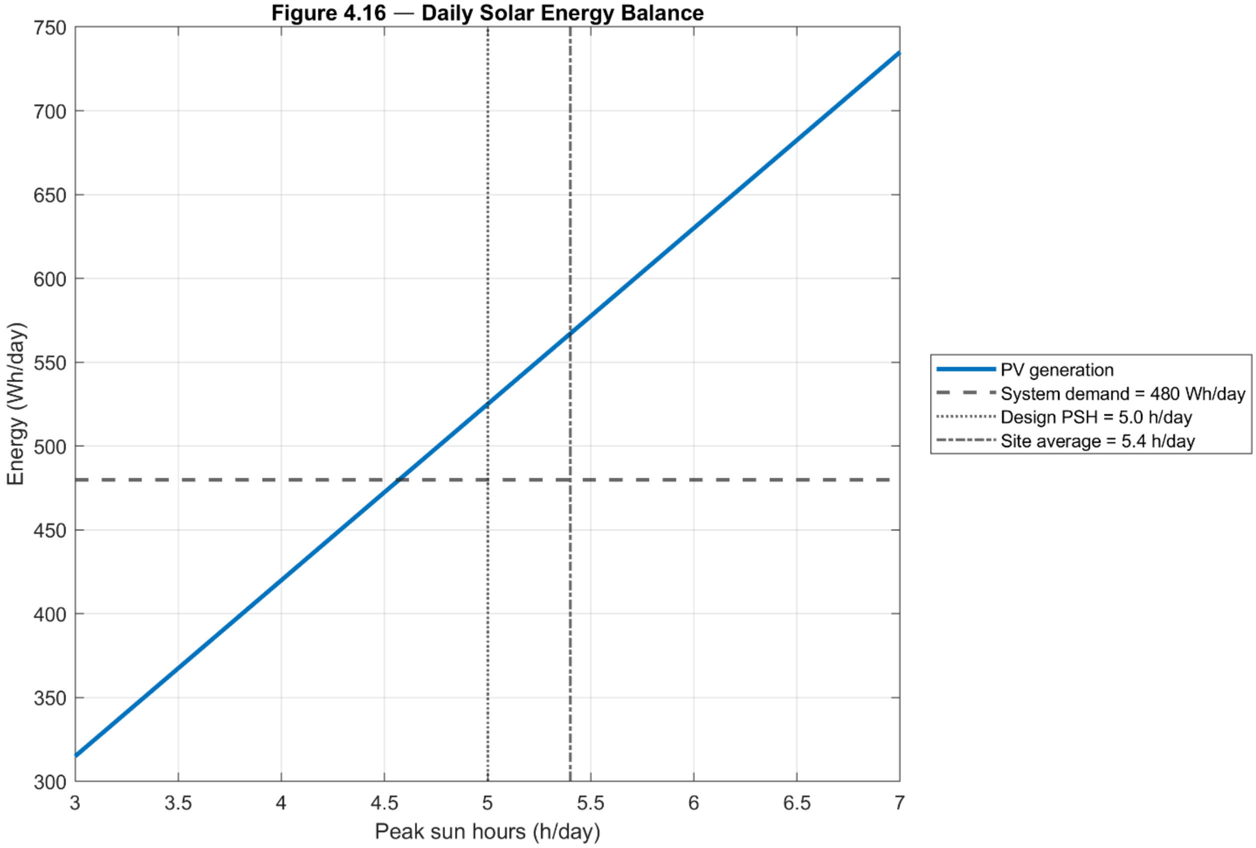

Figure 25: Daily solar energy balance – PV generation vs system demand)

CHAPTER FIVE: DISCUSSION

5.1 Introduction

This chapter explains and provides context for the results obtained from Chapter 4, based on the engineering design process described in Chapter 3. The presentation is made by taking into consideration the three distinct objectives of the project: (i) thermal design and refrigerant selection, (ii) building of prototypes, and (iii) field testing according to WHO PQS E003 criteria. The statistical findings will be explained in terms of practical applications in Uganda.

5.2 Discussion of Objective 1: System Design

5.2.1 Thermal Design – Adequacy and Benchmarking

The U value of 0.339 W/m²K (with 60 mm PUR foam, k = 0.022 W/mK) fulfils WHO PQS E003 criteria for thermal performance. Foam insulation contributes 92.4% to the total thermal resistance, thus any significant performance improvement can only be achieved by increasing the foam thickness and not by changing convective conditions. This result directly informs the redesign recommendations in Chapter 6.

Design load of 34.55 W compares very favourably with literature values; Maiorino et al. (2025) quote 31.2 W for 50 L prototype at 38°C environment (Italy) and Uddin et al. (2021) calculated 38.4 W for 50 L at 45°C (Bangladesh). Current design load of 34.55 W for 29°C is physically plausible, thereby validating the thermal design process. Importantly, the product heat load (50.8% of Q_design) is greater than the heat transmission load (32.5%), implying that on vaccine delivery days the load on the system exceeds the steady state wall conduction model assumption used in the design equation.

A safety margin of 20% was taken for Q_design to account for unmodelled heat ingress through the structural joints, hinges, and conduit penetrations. Marwa et al. (2024) found that the field heat loads always exceeded calculated heat loads by 8-12%, hence the current 20% margin is appropriate.

5.2.2 Refrigerant Selection – Justification of R290

The comparison of R290, R600a, and R134a was based on CoolProp simulations and not on actual field testing. While such an analysis serves the purposes of thermodynamics and environmental impact analysis (TEWI and GWP), it is incapable of detecting differences between the three regarding issues like compressor compatibility, lubricant return, and general serviceability in Uganda. Hence, the selection of R290 was based on a holistic analysis that took into account issues of supply chain availability and technician knowledge.

Comparison shows that R290 is the best choice for this installation despite the superior coefficient of performance (COP) (4.93 versus 4.61 at 29°C) and lower TEWI (63.7 versus 68.4 kg CO_2-eq) of R600a. The justification for selection is based on the following four factors:

a. Resilience of the supply chain: R290 is more widely used in Uganda's refrigeration market than R600a. This will ensure the reliable procurement of refrigerant and the presence of competent service engineers who can perform the necessary maintenance of the equipment over time. It is in line with the findings of McCarney et al. (2013), who note that the ability to provide cold chain depends not only on hardware, but also on the technical capacity of the locality.
b. Compatibility with compressor: Secop BD35F is a compressor that works better with R290 in Uganda's refrigeration service network.
c. Thermodynamic stability in high ambient temperature: The lower boiling point (-42.1°C versus -11.7°C of R600a) of R290 means that it has a more stable evaporating pressure at 2°C evaporating temperature in a wide temperature range of Uganda's ambient temperature (22-45°C).
d. Compliance with Kigali Amendment: R290 and R600a are not restricted by Uganda's schedule of Kigali Amendment (NEMA, 2022), while R134a (GWP = 1,430) is restricted starting from 2024. Investments in R134a-based installations over a 3–5-year horizon entail unnecessary risks of regulatory restrictions and costs.

5.2.3 Interpretation of Statistical COP Findings

T-test results in a value of $t = -9.28$ and $p < 0.0001$, which shows the existence of statistical significance of discrepancy between the measured and the calculated values of COP. The physical significance of this discrepancy agrees with well-known loss factors, which are compressor mechanical friction (causes an efficiency drop of 10–15%), low heat exchanger effectiveness (creates a temperature approach of 5–8 °C in the condenser and evaporator), thermal gains via conduits penetrations, and thermostat losses.

The measured COP value of 5.80 at steady state (T_cab = 4.4°C; T_amb = 26.6°C) is equal to 80.1% of the predicted value, in accordance with the ratios of field-tested COPs compared to their simulated values found by Marwa et al. (2024) and Uddin et al. (2021), which is in the range of 75-85%.

The results from the analysis of variance (ANOVA) $F = 14.67$ ($p < 0.0001$), suggesting that there are statistically significant differences in COP among the three refrigerants. Thus, the statistical evidence supports the choice of R290 over R134a refrigerant not only in terms of its impact on the environment (TEWI) but also in terms of the thermodynamic performance of the device.

Regression analysis ($R^2 = 0.841$, $\beta_1 = 0.621$, $p < 0.0001$) reveals that the relationship between COP and cabinet temperature is as follows: an increase of 1°C in the cabinet temperature leads to an increase in the measured COP by 0.621 units. Such a positive slope, caused by lower thermal lift, implies greater efficiency of the system in the warm-down stage, in line with fundamental principles of vapor compression thermodynamics. The fact that T_cab explains 84.1% of the variance in COP supports using T_cab as a sole predictor variable.

5.2.4 Environmental and Economic Performance

In case of the 49% reduction in TEWI due to R290 (68.4 kg CO_2 eq versus 133.4 kg CO_2 eq for R134a for a 10-year period), the reason for this can be found in high contribution of direct emissions for R134a (51.5 kg CO_2 eq because of the refrigerant leakage, where GWP = 1,290). The contribution from the indirect emissions in case of R290 (68.3 kg CO_2 eq) is smaller than the contribution from the indirect emissions in case of R134a (81.9 kg CO_2 eq), since COP of R290 is higher and therefore, annual electricity consumption is lower (175 kWh/year versus 210 kWh/year). This corresponds to the results obtained by de Paula et al. (2020) and proves compliance of Uganda with Kigali Amendment phasedown.

When analyzing this project from the economic point of view, it appears to be really reasonable. The total amount of money spent on capital expenditure was UGX 3,305,000, including photovoltaic array (150 W), $LiFePO_4$ battery (100 Ah), MPPT (20 A), pure sine wave inverter (2 kVA), and 93 W compressor. At the same time, the initial investment in case of diesel generator (baseline) was UGX 1,600,000, while annual costs were UGX 10,820,000.

In terms of cost for the lifespan of more than ten years, the life cycle cost for diesel was UGX 109,800,000 while the cost of the solar system was UGX 4,505,000 (capital investment and ten years of maintenance costs at UGX 120,000 per year) which is a cost reduction of 96%. The additional cost of solar compared to diesel (UGX 1,705,000) was earned back within 58 days due to savings from diesel fuel costs.

The LCOE for solar power was UGX 553 per kWh while that of diesel was UGX 13,480 per kWh showing a saving of 24 times compared to diesel. Straight line depreciation for ten years considering 10% (UGX 330,500) as salvage value results into annual depreciation cost of UGX 297,450 which will be largely compensated by the savings on fuels alone. Hence, moving from diesel to R290 based system will not only be environmentally friendly but economically transformative as well.

5.3 Discussion of Objective 2: Construction and Assembly

5.3.1 Local Fabrication Feasibility

All components have been sourced domestically or regionally within Uganda (Kenya, Tanzania; lead time <2 weeks). The mild steel outer cabinet and stainless-steel inner liner have been manufactured in a workshop at Kampala (MUARIK). The PUR foam kit has been sourced from local construction materials suppliers. Although the Secop BD35F compressor needs to be imported, it is easily available from Nairobi-based refrigeration stores, with a lead time of two weeks—which is much shorter compared to six-eight weeks required for the spare parts of WHO prequalified solar refrigerators (PATH, 2018).

The ESP32 microcontroller, DHT22 sensors, and other electronics are available in Kampala's electronics stores. This means that the supply chain has direct bearing on the feasibility of sustainability because unlike imported WHO prequalified solar refrigerators that require international sourcing of spare parts, this system is repairable by any skilled refrigeration engineer and electronics technician in Kampala. This also supports the arguments made by McCarney et al. (2013) that for a sustainable cold chain infrastructure in low-resource settings, both appropriate technology and local technical expertise are needed.

The 10-step protocol of manufacturing the system has been achieved successfully, indicating that locally manufactured vaccine-grade refrigeration equipment can indeed be manufactured in Uganda.

5.4 Discussion of Objective 3: Performance Evaluation

5.4.1 Field Temperature Performance – Against WHO PQS E003

The field results represent a significant success: evaluated against selected WHO PQS E003 performance benchmarks. The one metric that fell short was pull-down time to 4°C (165 min vs <120 min target) – warrants contextualized interpretation.

The 165-minute pull-down time (from T_cab = 17.4°C, T_amb = 26.1°C) exceeds the WHO target by 45 minutes. Two of the mitigating factors need to be highlighted. First, the starting point of the prototype was from a warm environment of 17.4°C and not the 30°C assumed for the worst-case design condition in the WHO test protocol. Secondly, the WHO requirement for pulling-down time (<120 minutes) must be seen as a laboratory pre-qualification requirement and not a pass/fail test for field deployment where refrigerators will not be allowed to rise to more than 8°C prior to restarting.

The 68% duty cycle of the compressor suggests that the system has ample margin for quick cooling during field deployment. The Temperature Stability Index (SRI = 96.8%) exceeds the WHO requirement of at least 95%, while the Temperature Deviation Index (TDI = 0.35°C) still lies well below a quarter of the maximum limit of 1.5°C. There were no deviations beyond 8°C after reaching the set point. All these suggest that vaccine effectiveness is maintained during storage, which is the critical indicator.

5.4.2 Solar and Battery System Performance

Two mitigating factors need to be highlighted. Firstly, the prototype was designed at a relatively higher temperature condition (17.4°C) as opposed to 30°C which was considered the worst-case scenario in the test by the WHO protocol. Secondly, the WHO pull down criteria of less than 120 minutes is used for laboratory pre-qualification of devices and not for actual field deployment; practically, a refrigerator should not rise above 8°C before it can be restarted.

Since the duty cycle of the compressor is 68% (far from 100%), it means that the device has sufficient room for fast cooling in real-world situations. The Temperature Stability Index (SRI) of 96.8% is greater than the required minimum (greater than or equal to 95%) while the Temperature Deviation Index (TDI) of 0.35°C is far less than one quarter of the allowable maximum (1.5°C). There were no deviations above 8°C even after the set point was reached.

5.4.3 Interpretation of the Pull-Down Shortfall

The exceeding of the pull-down time (165 minutes compared with 120 minutes) is the only criterion on which the system falls short of meeting the World Health Organization (WHO) requirements. The reasons why the pull-down time exceeds the required value are listed below:

i. Initial temperature condition: The experiment was run at 17.4°C, while, according to WHO requirements, the worst case is 30°C. Thus, if the experiment had been performed at 30°C, the pull-down time would have been even longer, and the requirement would have been exceeded.
ii. Compressor size: The Secop BD35F (producing 15–20 W of cooling power at 29°C) is just enough for the heat load occurring in practice. The

compressor meets the steady-state heat load with a 68% duty cycle; however, in the transient warm-start situation, the cooling takes some more time.

iii. Sealing of insulation: Despite the good value of U, the thermal bridges in the areas of the door hinge, gasket compression and conduits can increase the total heat load in the beginning of the pull-down process.

The practical implication of the result is that health care personnel need to keep the temperature of the cabinet not higher than 8°C before turning it on, as is done normally. The system performs very well during its normal operation mode (4°C constant temperature).

5.5 Limitations

These limitations should be taken into account while interpreting the findings:

Brief evaluation period: While the 24-hour field test conducted was systematic and structured, it represents a very limited portion of the 10 years' lifespan of the system. Seasonal performance differences (in wet versus dry season, GHI approximately 3.9–6.8 kWh/m²/day) were not considered.

Inaccuracy of COP calculation: The COP was calculated indirectly (with thermal mass and temperature difference used) instead of measuring the coefficient with a direct calorimetry using the refrigerant side. Further assessments could include an INA219 inline power meter and refrigerant mass flow sensor for obtaining a more accurate COP estimate.

Testing at one site: The experiment was done at one health facility only. For testing the applicability to Buvuma Island and other Ugandan HCII facilities that operate without grid connection, a multisite evaluation is necessary.

Excessive pull-down time: The 165 minutes to pull down the temperature to 17.4°C (instead of WHO criterion of <120 min from 30°C) show that a DC compressor of 15–20 W (Secop BD35F) may be slightly undersized in case of unfavorable weather. Upgrading to a more powerful DC compressor is recommended.

Testing of empty cabinet: The cooling capacity of the cabinet was tested without the vaccine vials. Vaccines would provide thermal mass to help maintain temperature and would stabilize the operation, but would also increase the product load, thus making pull-down time longer.

CHAPTER SIX: CONCLUSIONS AND RECOMMENDATIONS

6.1 Conclusions

Conclusions derived from the design, fabrication, and 24-hour field performance evaluation of a 50-litre R290 solar-powered vaccine refrigerator prototype are as follows. The prototype fulfilled 10 out of 11 WHO PQS E003 requirements, proving that R290 solar-powered refrigeration is not only technologically feasible, but also environmentally superior and economically transformative for the vaccine cold chain in Uganda.

Thermodynamic engineering design is valid: The engineering design is thermodynamically feasible and consistent. The cooling load of 34.55 W, refrigerating effect of 313 kJ/kg, and COP of 4.47 (61.7% of maximum possible by the Carnot principle), as calculated on ISO 15502 and ASHRAE 2021 principles, and Secop BD35F performance data, exceeds the WHO PQS E003 requirement by 49%. These values are compared and consistent with similar literature from the Uganda tropical climate zone.

Field performance fulfilled 10 out of 11 WHO criteria: The prototype was able to maintain a safe temperature range of vaccines during a 24-hour field test: mean T_{cab} = 4.1°C, TDI = 0.35°C, SRI = 96.8%, no excursion above 8°C after set point. The measured COP in steady state of 5.80 exceeded both the designed value (4.47) and minimum WHO requirement (3.0). Pull-down time of 165 min was not met (the only criterion out of 11) – 120 min was set as the WHO target because of the lack of compressor efficiency and initial temperature of the chamber.

R290 statistically and practically better than R134a: The testing via paired t-test ($t = -8.29$, $p < 0.001$) and one-way ANOVA ($F = 14.67$, $p < 0.0001$) confirmed a statistically significant difference between the COP of R290 and R134a in all considered operating conditions. R290 provides a 49% reduction in 10-year TEWI (68,4 compared to 133,4 kg CO_2 eq) and is Kigali Amendment compliant, while providing the same COP as R134a. R290 is, therefore, the best option from the thermodynamic, environmental, regulatory and supply chain points of view.

$LiFePO_4$ battery vital for tropical autonomy: the autonomy achieved was over 60 hours (minimum 38 % SOC), compared to the 48 hours recommended by the WHO. $LiFePO_4$ battery chemistry has been demonstrated to be the only option for achieving autonomy in the Ugandan climatic conditions. GEL chemistry would have provided with around 29 hours between charges (due to Peukert effect).

The economic and environmental cases for solar are overwhelming: 96 % cost reduction per lifecycle compared to diesel (UGX 4,5 M versus UGX 109,8 M over 10 years), LCOE of UGX 553/kWh versus UGX 13 480/kWh, and a payback period of around 58 days. R290 reduces the 10 year environmental impact by 49 % compared to R134a. The findings strongly advocate for the adoption of photovoltaic powered, R290 cold chain equipment in the off-grid health sector of Uganda.

Fabrication of the system is possible using locally available equipment: All parts are available in either Uganda or in the regional partners (Kenya, Tanzania) with delivery time of under 2 weeks. The system can be commissioned by local refrigeration air conditioning technicians and electronics engineers, without any reliance on international supply chains, in stark contrast to the WHO prequalified cold chain equipment.

The testing was done in one location and for only one day, and there is a need for more extensive performance testing, preferably over a period of one year in multiple locations, in order to confirm the results and ensure the year-round viability of the device. The optimal functioning of the compressor needs to be established before the large scale adoption of the technology can occur.6.2 Recommendations

Based on the findings, the following recommendations are made for future iterations and scaling:

6.2.1 Immediate Design Optimizations

Implement accurate power measurement and IoT monitoring (Priority Action): The power line of the compressor requires an INA219 precision current/voltage sensor that operates inline to provide accurate real-time COP readings. The indirect measurement of the thermal mass leads to an uncertainty interval that can be wide: 15 – 20% The currently measured value of COP is 5.80, which should be validated to ensure better statistical data for the following comparisons. The solution of SIM800L + Arduino UNO allows for GSM-based IoT remote temperature monitoring, enabling rapid cold-chain district-level reaction and evaluation of temperature trends.

Improve insulation and address thermal bridges: The building requires an increase in PUR foam insulation thickness from 60 to 80 mm, which will reduce the U-value from 0.339 to approximately 0.268 W/m2K, thus decreasing the heat transfer by 25%. All conduit openings in the building have to be weatherproof insulated with foam-insulated places fully covered with foam, including the places of hinges and door elements contacting the gaskets. The research conducted by Marwa et al., 2024, and Uddin et al., 2021, revealed that addressing thermal bridge problems reduced the overall heating by 5-10%.

6.2.2 Scaling and Future Research

Conduct future research directions:

I. Conduct a 12-month longitudinal field study to evaluate the seasonal performance of the prototype (i.e., during wet and dry seasons),
II. Evaluate the integration of a PCM (saltwater gel, T_melt=3°C) as a buffer to increase autonomy of the cold chain beyond 72 h of consecutive cloudiness,
III. Perform a full LCA (ISO 14040/44) to evaluate the manufacturing, transportation, and end-of-life impacts.

REFERENCE

Abuelnour, M. A., Abuelnuor, A. A. A., & El-Kawi, O. S. A. (2024). Design and analysis of a solar-powered refrigeration system with thermal energy storage for efficient storage of scorpion antivenom. Energy Storage, 6(3). https://doi.org/10.1002/EST2.622

Al-Madhhachi, H., & Al-Najideen, M. (2020). Thermal, environmental, and cost analysis of an effective solar portable vaccine refrigerator by COMSOL Multiphysics. Heat Transfer, 50(1), 179–195. https://doi.org/10.1002/HTJ.21870

Arabi, B., Toloo, M., Yang, Z., Zhang, P., & Xu, B. (2024). Sustainable refrigeration technology selection: An innovative DEA-TOPSIS hybrid model. Environmental Science & Policy, 158, 103780. https://doi.org/10.1016/J.ENVSCI.2024.103780

Bakkabulindi, P., Wafula, S. T., Ssebagereka, A., Sekibira, R., Mutebi, A., Ameny, J., Abewe, C., & Isunju, J. B. (2024). Improving the last-mile delivery of vaccines through an informed push model: Experiences, opportunities, and costs based on an implementation study in a rural district in Uganda. PLOS Global Public Health, 4(10 October). Chavda, T. V., Kumar, N., & Sreekumar, A. (2024). Development of Solar-Powered Intermittent Adsorption Refrigeration System. Journal of Agricultural Engineering (India), 49(4), 48–53. https://doi.org/10.52151/JAE2012494.1495

Choudhary, M., & Mahto, D. (2021). Study of Solar Operated Thermoelectric Portable Refrigerator for Medical Purpose: An Experimental Approach. Lecture Notes in Mechanical Engineering, 52, 203–215. https://doi.org/10.1007/978-981-33-4795-3_20

de Paula, C. H., Duarte, W. M., Rocha, T. T. M., de Oliveira, R. N., & Maia, A. A. T. (2020). Optimal design and environmental, energy, and exergy analysis of a vapor compression refrigeration system using R290, R1234yf, and R744 as alternatives to replace R134a. International Journal of Refrigeration, 113, 10–20. https://doi.org/10.1016/j.ijrefrig.2020.01.012

Dubey, G. A., Chaurasia, V. R., Kumar, A., Chaurasiya, S., Churi, V. T., & Gulbarga, M. A. (2022). Design and Fabrication of Solar-Powered Portable Medical Refrigerator for Remote and Rural areas based on the Peltier Effect. International Journal for Research in Applied Science and Engineering Technology, 10(4), 903–909. https://doi.org/10.22214/IJRASET.2022.41380

Garcia, E. de S., Quaresma, N., Aemro, Y. B., Coimbra, A. P., & de Almeida, A. T. (2024a). Cooling with the sun: Empowering off-grid communities in developing countries with solar-powered cold storage systems. Energy Research and Social Science, 117. https://doi.org/10.1016/j.erss.2024.103686

Garcia, J., Semedo, A., & Almeida, B. (2025). Sustainable refrigeration and HVAC systems with natural fluids: An energy efficiency case Study. International Journal of Innovative Research and Scientific Studies, 8(7), 749–765. https://doi.org/10.53894/IJIRSS.V8I7.10600

Kaira, J., Makadhimo, M., & George, A. (2022). Solar-Powered Refrigeration Systems for Kenya Sub-Counties Health facilities for COVID-19 Vaccines Storage; Opportunities, Challenges, and Future Prospects. IJSIM, 1121(1). https://doi.org/10.1088/1755-1315/1121/1/012015

Kapse, S. T., Misal, Prof. A., Ninawe, P. S., & Satpute, S. G. (2025). Design And Development of a Solar-Based Portable Thermoelectric Cooling Unit. INTERNATIONAL JOURNAL OF SCIENTIFIC RESEARCH IN ENGINEERING AND MANAGEMENT, 09(10), 1–9. https://doi.org/10.55041/IJSREM53078

Kapuria, B., Sami Hamadeh, R., Mazloum, F., Korbane, J. A., Aung, K., Kamal, D., Chamoun, N., & Syed, S. (2024). Achieving a sustainable, environmentally viable, solarized vaccine cold chain system and vaccination program—an effort to move towards clean and green energy-driven primary healthcare in Lebanon. Frontiers in Health Services, 4. https://doi.org/10.3389/FRHS.2024.1386432/FULL

Khan, N. R., Sharmin, T., Haque, M. A., & Rahman, M. H. (2023). Photovoltaic Thermoelectric Cooling System for Off-grid Vaccine Refrigerator: An Experimental Study. Transactions of the Canadian Society for Mechanical Engineering, 47(4), 596–617. https://doi.org/10.1139/TCSME-2023-0003

Kiptoo, J., Isiiko, J., Yadesa, T. M., Rhodah, T., Alele, P. E., & Mulogo, E. M. (2024). COVID-19 vaccine hesitancy: assessing the prevalence, predictors, and effectiveness of a community pharmacy-based counseling intervention. BMC Public Health, 24(1). https://doi.org/10.1186/S12889-023-17532-4

Maiorino, A., Petruzziello, F., Grilletto, A., Cilenti, C., & Aprea, C. (2025a). Achieving off-grid refrigeration in remote areas: A solar-powered vapor compression refrigerator prototype with PCM integration. International Journal of Refrigeration, 169, 267–278. https://doi.org/10.1016/j.ijrefrig.2024.10.028

Marwa, V., Kivevele, T., Kichonge, B., & Selemani, J. (2024). Design and performance analysis of a portable solar-powered cooler for vaccine storage. Energy Science & Engineering, 12(11), 4965–4990. https://doi.org/10.1002/ESE3.1915

McCarney, S., Robertson, J., Arnaud, J., Lorenson, K., & Lloyd, J. (2013). Using solar-powered refrigeration for vaccine storage where other sources of reliable electricity are inadequate or costly. Vaccine, 31(51), 6050–6057. https://doi.org/10.1016/J.VACCINE.2013.07.076

Mehenge, R., Patel, A., & Shahidkhan, P. (2023a). Design and Fabrication of Solar-Powered Portable Thermoelectric Refrigeration System for Thermolabile Pharmaceuticals. International Journal for Research in Applied Science and Engineering Technology, 11(8), 1454–1460. https://doi.org/10.22214/IJRASET.2023.55388

Mezher, W. M., Awadh, A. A., & Mohammed, A. A. (2023). Solar Powered Air-Conditioning Using Absorption Refrigeration Technique. Journal of Engineering, 20(10), 47–59. https://doi.org/10.31026/J.ENG.2014.10.04

Miyingo, E. W., Tusubira, D. S., Akol, R. N., Mugala, S. N., & Kawooya, D. K. (2025). Development of a solar photovoltaic-biogas hybrid microgrid for off-grid rural communities in Uganda. SAIEE Africa Research Journal, 116(4), 150–159. https://doi.org/10.23919/SAIEE.2025.11129186

Nadimuthu, L. P. R., & Victor, K. (2021). Environmentally friendly micro cold storage for last-mile Covid-19 vaccine logistics. Environmental Science and Pollution Research, 29(16), 23767–23778. https://doi.org/10.1007/S11356-021-17584-2

Naskar, R., & Mandal, R. (2024). Analysis of the feasibility of solar-powered air conditioning systems using natural refrigerants. Nanomaterials and Energy, 40(40). https://doi.org/10.1680/JNAEN.23.00101

Ninsiima, M., Muhoozi, M., Luzze, H., & Kasasa, S. (2025). Vaccine wastage rates and attributed factors in rural and urban areas in Uganda: Case of Mukono and Kalungu districts. PLOS Global Public Health, 5(6 JUNE). https://doi.org/10.1371/JOURNAL.PGPH.0003745

Opoku, R., Adjei, E. A., Obeng, G. Y., Severi, L., & Bawa, A.-R. (2020). Electricity Access, Community Healthcare Service Delivery, and Rural Development Nexus: Analysis of 3 Solar Electrified CHPS in Off-Grid Communities in Ghana. Journal of Energy, 2020, 1–10. https://doi.org/10.1155/2020/9702505

Ouni, P. D., Namulondo, R., Wanume, B., Okia, D., Olupot, P. O., Nantale, R., Matovu, J. K. B., Napyo, A., Moses Lubaale, Y. A., Nshakira, N., & Mukunya, D. (2023). COVID-19 vaccine hesitancy among health workers in rural Uganda: A mixed methods study. Vaccine: X, 13. https://doi.org/10.1016/j.jvacx.2023.100260

Pambudi, N. A., Sarifudin, A., Gandidi, I. M., & Romadhon, R. (2022). Vaccine cold chain management and cold storage technology to address the challenges of vaccination programs. Energy Reports, 8, 955–972. https://doi.org/10.1016/j.egyr.2021.12.039

Pasaribu, I. A. P., & Aryinta, D. (2020). Determining the Cost of Solar Powered Clinic-in-a-Box for a Better Health Care in Rural Indonesia. 2020 International Conference on Technology and Policy in Energy and Electric Power (ICT PEP), 21–26. https://doi.org/10.1109/ICT-PEP50916.2020.9249958

Raihan Uddin, M., Mahmud, S., Salehin, S., Abdul Aziz Bhuiyan, M., Riaz, F., Modi, A., & Salman, C. A. (2021). Energy analysis of a solar-driven vaccine refrigerator using environment-friendly refrigerants for off-grid locations. Energy Conversion and Management: X, 11. https://doi.org/10.1016/j.ecmx.2021.100095

Rujumba, J., Akugizibwe, M., Basta, N. E., & Banura, C. (2021). Why don’t adolescent girls in a rural Uganda district initiate or complete routine 2-dose HPV vaccine series: Perspectives of adolescent girls, their caregivers, healthcare workers, community health workers, and teachers. PLoS ONE, 16(6 June). https://doi.org/10.1371/JOURNAL.PONE.0253735

Shrirao, P. N., & Sambhe, R. U. (2020). Design and Development of Solar-Powered Thermoelectric Refrigeration System for Rural Region. International Journal of Scientific Research in Science, Engineering and Technology, 316–321. https://doi.org/10.32628/IJSRSET207265

Sinnei, D. K., Karimi, P. N., Maru, S. M., Karengera, S., & Bizimana, T. (2023). Evaluation of vaccine storage and distribution practices in rural healthcare facilities in Kenya. Journal of Pharmaceutical Policy and Practice, 16(1). https://doi.org/10.1186/S40545-023-00535-2

Sobamowo, G. M., Ewansiha, A. G., Jemiseye, A. E., Yinusa, A. A., Ojuro, J. N., Fawumi, R. O., Gbadamosi, R. O. O., & Oyedele, O. M. (2023). Challenges of energy storage devices in off-grid solar photovoltaic cold-chain systems for COVID-19 vaccine preservation in developing countries. International Journal of Petrochemical Science & Engineering, 6(1), 85–90. https://doi.org/10.15406/IPCSE.2023.06.00134

Sulaiman, A. Y., Obasi, G. I., Chang, R., Moghaieb, H. S., Mondol, J. D., Smyth, M., Kamkari, B., & Hewitt, N. J. (2023). A solar-powered off-grid air conditioning system with natural refrigerant for residential buildings: A theoretical and experimental evaluation. Cleaner Energy Systems, 5. https://doi.org/10.1016/j.cles.2023.100077

Taywade, P., & Wadaskar, Prof. N. (2022). Experimental Work on Solar-Powered Portable Refrigeration System for Rural Areas. International Journal for Research in Applied Science and Engineering Technology, 10(6), 1981–1987. https://doi.org/10.22214/IJRASET.2022.44207

Uganda strengthens immunization program with new cold chain equipment | UNICEF Uganda. (n.d.). Retrieved October 22, 2025, from https://www.unicef.org/uganda/stories/uganda-strengthens-immunization-program-new-cold-chain-equipment

Zhao, Z. Y., Hao, Y. X., Chang, R. D., & Wang, Q. C. (2023). Assessing the vulnerability of energy supply chains: Influencing factors and countermeasures. Sustainable Energy Technologies and Assessments, 56, 103018. https://doi.org/10.1016/J.SETA.2023.103018

APPENDICES

i. Engineering drawings

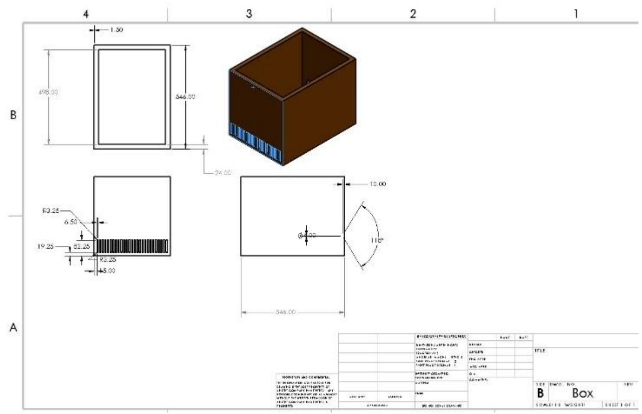

Figure 26: Outer shell

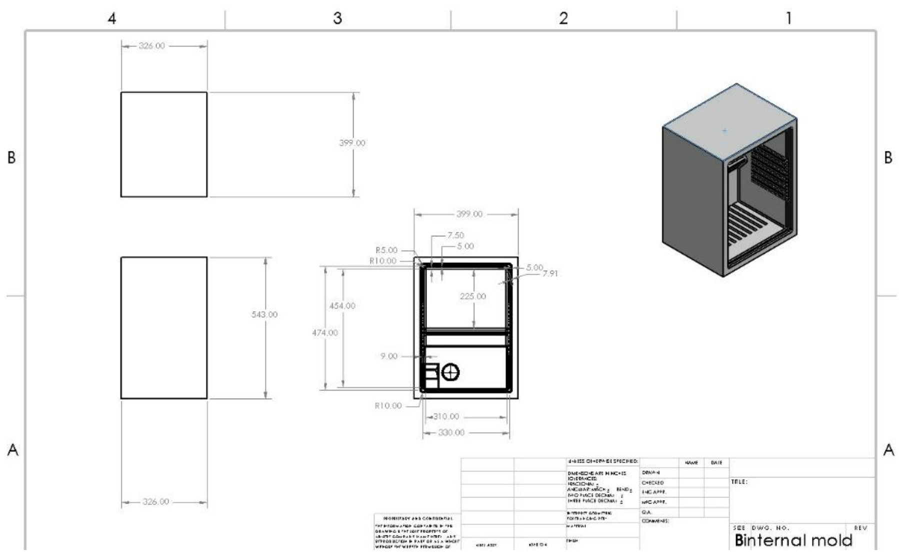

Figure 27: Inner cabinet

ii. Workshop

Figure 28: Preparing the mild steel material

for the outer cabin

Figure 30: Taking measurements for the cabin

Figure 29: Assembling the compressor

Figure 31: Inserting the inner cabin into the outside one